A Noetherian approach to invariants for the statics and dynamics of elastic rods

Sébastien Neukirch[a,*], Florence Bertails-Descoubes[b]

[a] *Sorbonne Université, CNRS, Institut Jean Le Rond d'Alembert, F-75005 Paris, France*
[b] *Univ. Grenoble-Alpes, INRIA, CNRS, Grenoble INP, LJK, France*

Abstract

The static-dynamic analogy discovered by G. Kirchhoff shows that the statics of an elastic beam is equivalent to the dynamics of a spinning top. This analogy, where time and angular velocity are, for example, equivalent to arclength and curvatures, allows the use of Noether's theorem to unravel a quantity that is invariant along elastic rods at equilibrium. A spinning top having a Lagrangian independent of time will have its mechanical energy constant in time. In the same manner, an elastic rod with uniform elastic properties will have the sum of its curvature energy and its tension force uniform along the structure. The invariant property is known in simple cases, but the present approach generalises it to more complex cases where extensibility, shear, conservative loads (e.g. gravity), and contact are involved. Moreover, still using Noether's theorem and bringing to light the continuous symmetries of the Lagrangian of the variational approach, we recover all known invariants for the statics and dynamics of rods and ribbons, and we extend the approach to vibrations. Finally, we show how the arclength invariant may be used to sometimes obtain pivotal information on elastic rod problems or to test the accuracy of numerical codes.

Keywords: elastic rods, Hamiltonian and Lagrangian formulations, contact

1. Introduction

The discovery of a conserved quantity while studying a dynamical system is generally a joyful event for the researcher as it usually brings new insights into the system's behavior. In her PhD thesis, the German mathematician Emmy Noether meticulously derived more than 300 invariants for biquadratic systems (Noether, 1908). These invariants were explicitly calculated by hand, possibly through trial and error, and later on, E. Noether passed a harsh judgment on her PhD work and oriented her studies toward abstract algebra (Dick, 1981, p. 17). Nevertheless, her Habilitation thesis contains the classic 1918 theorem on differential invariants which provides a systematic way of unravelling invariants in physics and mechanics problems (Noether, 1918) and was most probably initiated in relation with the variational approach of Einstein's general theory of relativity (Dick, 1981, p. 36).

Noether's theorem states that if the Action (of Lagrangian mechanics) stays the same when a translation, rotation, or some other space or time transformation is performed, then a given quantity will be invariant during the dynamics of the system. The best-known case is the invariance of the mechanical energy of a system if the Lagrangian of this system does not explicitly depend on time, and thus remains the same through a translation in time. In this paper, we leverage this theorem for the statics and dynamics of elastic rods to recover all their known invariants, thereby providing the corresponding space transformations responsible for these invariants. We additionally generalise the invariants to the case where a conservative force field is applied to the rod, as well as frictionless contact. Finally, we provide several illustrative examples where the arclength invariant is shown to be particularly handy in the study of the mechanics of the system.

*Corresponding author
Email address: sebastien.neukirch@cnrs.fr (Sébastien Neukirch)

State of the art

Variational approaches of rods. In mechanical engineering, variational approaches of rods have long been motivated by the design of Galerkin-type numerical methods, especially finite elements. A popular method is the so-called geometrically exact beam approach (Reissner, 1973; Simo and Vu-Quoc, 1986), which derives an exact weak formulation for a generalised (Timoshenko) rod model including bending, stretching and shearing energies. The displacement and rotation fields are then discretised with the help of interpolating shape functions. One important issue of this approach (that is well beyond the scope of the present paper), which spurred many subsequent works in the finite elements community, deals with the proper interpolation of rotations for preserving *objectivity*, i.e., invariance of the strain measures under rigid motion (Crisfield and Jelenić, 1998).

The weak formulations exploited for finite elements generally rely on the *principle of virtual work*, which stipulates that the variation of internal energy of the system should be balanced by the work of external forces. One difficulty pertaining to the virtual work principle is the definition of virtual displacements that comply with the true kinematics of the system. For rods in particular, a concern deals with the parametrisation of rotations and the nature of coupling between positional (displacement of the centreline) and rotational (rotations of the material frame) degrees of freedom. Various parametrisations have been proposed for rotations, including Euler angles (O'Reilly, 2015, Section 5.3.1), quaternions (Dichmann et al., 1996), or the exponential map in the rotation group $\mathcal{SO}(3)$ (Simo and Vu-Quoc, 1986). Likewise, various classes of weak formulations have been introduced with different levels of coupling between virtual displacements in positions and rotations. Methods range from uncoupled (Reissner, 1973) and weakly coupled ones in $\mathbb{R}^n \times \mathcal{SO}(3)$ (Sonneville et al., 2014) for general (Timoshenko) beams, to fully coupled ones for inextensible Kirchhoff rods where only rotational (bending and twisting) degrees of freedom are considered (Audoly and Pomeau, 2010, Section 3.6). All these methods lead to the correct mechanical equations for the considered rod models, albeit at the price of properly defining the structure of the space where virtual displacements should live in.

An alternative variational method is the *principle of least action*, which stipulates that the *action* of the system – that is, in statics, the integral of the *Lagrangian* of the system over s – should be stationary. This principle leads to the so-called *Euler-Lagrange equations*, which are differential equations that should be satisfied by the degrees of freedom $q(s)$ of the system along with their derivatives $q'(s)$. Though mathematically equivalent to the virtual work principle for conservative systems, this approach is quite different in spirit. Instead of formulating virtual displacements and computing corresponding energy variations, it is sufficient to build a Lagrangian – an energy depending on $q(s)$ and $q'(s)$– that complies with the kinematics and mechanics of the system. In order to couple some degrees of freedom together, or to model contact, constraints can easily be incorporated in the Lagrangian. Then, the Euler-Lagrangian equations appear as a simple recipe to derive the mechanical equations of the system from the Lagrangian. Another key motivation to use the Lagrangian formalism is that Noether's theorem on invariants is best understood and derived from symmetries of the Lagrangian itself.

For these reasons, we shall adopt the Lagrangian point of view in this paper. To demonstrate the versatility of this approach, we will show that we can retrieve the same invariants for rods by considering two choices of degrees of freedom: on the one hand, simple (and totally uncoupled) degrees of freedom living all on $\mathbb{R}^n$, which are related to each other through external constraints; on the other hand, translational and rotational degrees of freedom living on the Lie group of rotations $\mathcal{SO}(3)$, which are coupled together through a single external constraint. We will also show that adding contact constraints is straightforward within this Lagrangian approach, and allows one to extend Noether invariants to systems in (frictionless) contact.

Hamilton point of view and invariants for rods. To study mathematical properties of rods and their invariants, theorists have often adopted an *Hamiltonian* point of view, that is, considered the Legendre transformation of the Lagrangian. Indeed, for conservative systems, the Hamiltonian naturally appears as an invariant, which actually boils down to the Noether invariant for a time-translational symmetry of the corresponding Lagrangian. For rods, different invariants have been found by analysing directly the Hamiltonian structure of the mechanical (strong) equations of the system (Maddocks and Dichmann, 1994).

Among these invariants, the static arclength invariant H, consisting in the sum of the bending energy, twist energy, and the tension (axial component of the internal force), stands apart. It was first mentioned in the book by Love (1944, p. 384, Eqn. (7) in Sect. 262), then discussed in (Maddocks and Dichmann, 1994), and later on thoroughly used by Maddocks and coworkers (Dichmann et al., 1996; Kehrbaum and Maddocks, 1997) where it appears as the

Hamiltonian in the 3D rods statics formulation. The jump conditions of these conservation laws have been studied in (O'Reilly, 2007) in the light of the Weierstrass–Erdmann corner condition, see also (O'Reilly, 2017).

It is noteworthy that these invariants were found using a trial-and-error approach, i.e. no systematic perspective was followed. As a matter of fact, such a systematic way exists: it relies on the Lagrangian and on Noether 1918's theorem (Noether, 1918), which states that each continuous symmetry of the Lagrangian, constructed from *both* the energy *and* the kinematic constraints of the system, calls for an invariant quantity. The Noether approach to the conserved quantities has been used in the general case of bulk linear elasticity (Olver, 1984) and different fluid and solid mechanics problems (Singh and Hanna, 2021). For rods however, a complete Noetherian view has seldom been adopted. Maddocks and Dichmann (1994) briefly mentioned the possible use of Noether's theorem to constructively find conservation laws, but rather used an a posteriori verification approach to the computation of the invariants, starting from the strong version of Kirchhoff's rod equations. Peng et al. (2013) used Noether's theorem but could not explicitly provide all known invariants because they did not introduce the continuous constraints in the Lagrangian. Overall, the fact that several invariants can be generalised to the case where a conservative force field is applied on the rod seems to have been overlooked in the literature, with the exception of self-weight, see (O'Reilly, 2015, 2017). Finally, contact was merely treated in the light of jump conditions (O'Reilly, 2007, 2017) where it was shown to help the computation of integration constants (Clauvelin et al., 2009).

The approach developed in this paper rationalises the construction of the invariants using a Lagrangian mechanics approach, and shows that the invariants can be computed systematically once all continuous constraints have been properly introduced in the Lagrangian, together with their corresponding multipliers. The case of pointwise and continuous (frictionless) contact is moreover shown to fit in naturally with the present Noetherian approach.

Paper contributions

- A simple and pedagogical derivation of the Reissner and Kirchhoff static and dynamic equations from the least action principle, with pointwise constraints, contact, and external conservative force fields.
- The application of Noether's formulas to retrieve and generalise all known invariants in the presence of frictionless contact and external conservative force fields, valid for Kirchhoff, Reissner, and elastic ribbon cases.
- The derivations of the results above using two alternatives: a simple Lagrangian formulation on $\mathbb{R}^n$ with multiple external constraints, and a more compact Lagrangian formulation on $\mathbb{R}^n \times SO(3)$ retaining only one single constraint.
- The illustration of the use of the arclength invariant H on several cases, including sliding sleeves, plectonemes, and constrained Euler buckling.
- The applications of invariants to the verification of numerical simulation codes.

2. Noether's theorem and extension to $\mathbb{R}^n \times SO(3)$

In the following, scalar quantities are printed with plain font, and vector quantities of $\mathbb{R}^n, n > 1$ with bold font. Matrices are represented with capital letters.

2.1. Emmy Noether's 1918 theorem

Let the generalised coordinates of the system $\boldsymbol{q} = \boldsymbol{q}(s,t)$ be functions from $\mathbb{R}^2$ to $\mathbb{R}^n$, and $' \equiv \partial/\partial s$, and $\dot{} \equiv \partial/\partial t$ be the space and time derivatives, respectively. For the sake of readability, in the following we may often drop the s, t dependencies, for instance writing $\boldsymbol{q}'$ instead of $\boldsymbol{q}'(s,t)$.

If the following action

$$\mathcal{A} = \int_t \int_s \mathcal{L}(\boldsymbol{q}, \dot{\boldsymbol{q}}, \boldsymbol{q}')\, ds\, dt \tag{1}$$

remains identical when the following transformations are performed,

$$\tilde{\boldsymbol{q}} = \boldsymbol{q} + \epsilon\,\boldsymbol{\theta}\,, \tag{2a}$$
$$\tilde{s} = s + \epsilon\,\sigma\,, \tag{2b}$$
$$\tilde{t} = t + \epsilon\,\tau \tag{2c}$$

with $|\epsilon| \ll 1$, and in particular if $\tilde{\mathcal{L}} = \mathcal{L}$, then the following relation

$$\left[\tau\,\mathcal{L} + (\boldsymbol{\theta} - \tau\dot{\boldsymbol{q}} - \sigma\boldsymbol{q}')\cdot\frac{\partial\mathcal{L}}{\partial\dot{\boldsymbol{q}}}\right]^{\bullet} + \left[\sigma\,\mathcal{L} + (\boldsymbol{\theta} - \tau\dot{\boldsymbol{q}} - \sigma\boldsymbol{q}')\cdot\frac{\partial\mathcal{L}}{\partial\boldsymbol{q}'}\right]' = 0\ \forall s\,, \forall t. \tag{3}$$

holds for dynamical solutions, i.e. for trajectories $\boldsymbol{q}(s,t)$ under which the action (1) is stationary (Noether, 1918). The three transformations do not have to occur simultaneously, i.e. we have (Noether, 1918)

$$\text{if } \tau = 0 \text{ and } \sigma = 0,\ \text{then } \tilde{\boldsymbol{q}} = \boldsymbol{q} + \epsilon\,\boldsymbol{\theta} \text{ and } \left[\boldsymbol{\theta}\cdot\frac{\partial\mathcal{L}}{\partial\dot{\boldsymbol{q}}}\right]^{\bullet} + \left[\boldsymbol{\theta}\cdot\frac{\partial\mathcal{L}}{\partial\boldsymbol{q}'}\right]' = 0\ \forall s\,, \forall t \tag{4a}$$

$$\text{if } \tau = 0 \text{ and } \theta = 0,\ \text{then } \tilde{s} = s + \epsilon\,\sigma \text{ and } \left[\boldsymbol{q}'\cdot\frac{\partial\mathcal{L}}{\partial\dot{\boldsymbol{q}}}\right]^{\bullet} + \left[-\mathcal{L} + \boldsymbol{q}'\cdot\frac{\partial\mathcal{L}}{\partial\boldsymbol{q}'}\right]' = 0\ \forall s\,, \forall t \tag{4b}$$

$$\text{if } \sigma = 0 \text{ and } \theta = 0,\ \text{then } \tilde{t} = t + \epsilon\,\tau \text{ and } \left[-\mathcal{L} + \dot{\boldsymbol{q}}\cdot\frac{\partial\mathcal{L}}{\partial\dot{\boldsymbol{q}}}\right]^{\bullet} + \left[\dot{\boldsymbol{q}}\cdot\frac{\partial\mathcal{L}}{\partial\boldsymbol{q}'}\right]' = 0\ \forall s\,, \forall t. \tag{4c}$$

Please note that $\boldsymbol{q}$ and its derivatives $\boldsymbol{q}', \dot{\boldsymbol{q}}$ are vectors of dimension n, and the gradients $\partial\mathcal{L}/\partial\boldsymbol{q}, \partial\mathcal{L}/\partial\boldsymbol{q}', \partial\mathcal{L}/\partial\dot{\boldsymbol{q}}$ are vectors of the same dimension n: scalar products arise between these two types of quantities.

Static case. In the particular static case where there is no time dependence, (4b) implies the most well-known part of Noether's theorem: if the *Lagrangian* $\mathcal{L}$ does not explicitly depends on s (but only does through $\boldsymbol{q}(s)$ and $\boldsymbol{q}'(s)$), then

$$H(s) = \boldsymbol{q}'\cdot\frac{\partial\mathcal{L}}{\partial\boldsymbol{q}'} - \mathcal{L}, \tag{5}$$

which corresponds to the *Hamiltonian* of the system, is a conserved quantity, i.e. $\forall s$, $H'(s) = 0$. In the following, this space invariant will thus be simply denoted by H.

Constraints. For the sake of simplicity, we only focus on the static case here again. We consider the system to be subject to a bilateral constraint of the form $h(\boldsymbol{q}, \boldsymbol{q}') = 0$, meaning that the generalised coordinates are not necessarily independent. The stationarity of the action under this constraint can be found by considering a constraint-free problem where the action is modified by transforming the Lagrangian as

$$\mathcal{L} \leftarrow \mathcal{L} - \lambda(s)\,h(\boldsymbol{q}, \boldsymbol{q}'), \tag{6}$$

where $\lambda(s)$ is the *Lagrangian multiplier* associated to the constraint $h(\boldsymbol{q}, \boldsymbol{q}') = 0$. The reader may think that introducing the multiplier $\lambda(s)$ to the Lagrangian adds an explicit dependence of $\mathcal{L}$ on the space variable s, hence jeopardising the validity of Noether's arclength invariant (5). However it can be shown that all the previous Noether invariants remain valid, including (5), due to the fact that $h(\boldsymbol{q}, \boldsymbol{q}') = 0$ at equilibrium.

Note that the new Lagrangian (6) does not contribute the $-\mathcal{L}$ part of Noether's invariant, as $h(\boldsymbol{q}, \boldsymbol{q}') = 0$ at equilibrium. However it may bring a new term of the form $\boldsymbol{q}'\cdot\frac{\partial\mathcal{L}}{\partial\boldsymbol{q}'}$ if the constraint h depends on $\boldsymbol{q}'$. In section 4, we show in particular that the tension of the rod emerges in the static rod invariant, precisely due to the kinematic constraint relating the rod centreline to its material frame.

2.2. *Noether's theorem on $\mathbb{R}^n \times SO(3)$*

In this section we limit ourselves to the static case. So far we have expressed Noether's theorem considering that $\boldsymbol{q}$ is a vector of $\mathbb{R}^n$, with the property that its derivative can simply be taken component-wise. This theorem naturally follows from the Euler-Lagrange equations on $\mathbb{R}^n$ (see Appendix A). However, key variables such as 3D rotations may not freely evolve in a full vector space, hence they may not be represented as three independent vectors of $\mathbb{R}^3$. Indeed, computing the derivative of a rotation matrix as derivatives of the matrix components (i.e. on $\mathbb{R}^3$) does not allow one to recover a rotation matrix after integration. Said otherwise, the resulting vector derivative is not tangent to the space of rotation matrices (the so-called $\mathcal{SO}(3)$ group). In 2D, this problem is easily solved by parametrising rotations with a scalar θ corresponding to the rotation angle about the horizontal axis. In such a case, rotation matrices do not need to be explicitly represented as variables, only the scalar variable $q = \theta$ and its derivatives θ' and $\dot{\theta}$ are sufficient, which brings us back to the (easy) vector case. Unfortunately, such a vector reduction is not straightforward in 3D.

In 3D, a first approach to tackle this problem is to consider external constraints applied onto $\boldsymbol{q}$ and inject them in the Lagrangian: this is what we will do in Sections 5 and 8, leveraging the property that Noether's invariants still hold in case of bilateral constraints, see above. This 'flattening' method has the advantage of being systematic and simple to apply, since one can still resort to the classical Euler-Lagrange equations and Noether's theorem on $\mathbb{R}^n$. However it requires formulating all kinematic constraints properly (especially constraints on $\mathcal{SO}(3)$), and burdens the user with a few tedious calculations. A second, more compact method consists in *reformulating* new Euler-Lagrange and new Noether equations, that are *valid on* $\mathcal{SO}(3)$. This is possible to do so by applying the so-called Euler-Poincaré reduction, which keeps track of rotation matrices R as main degrees of freedom, but considers their derivative to be a vector of $\mathbb{R}^3$, denoted by $\boldsymbol{u}$ in the world space, or $\bar{\boldsymbol{u}}$ in the local rotating space. Explicitly, if $R \in \mathcal{SO}(3)$, then R' reads

$$R' = [\boldsymbol{u}]_\times R = R\,[\bar{\boldsymbol{u}}]_\times \quad \text{with} \quad \boldsymbol{u} = R\,\bar{\boldsymbol{u}}, \tag{7}$$

where $[x]_\times$ stands for the cross-product matrix of vector $x \in \mathbb{R}^3$, such that $[x]_\times\, y = x \times y\,,\ \forall y \in \mathbb{R}^3$, see e.g. (Casati, 2015, Appendix D) for practical computations on $\mathcal{SO}(3)$.

It is noteworthy that with such a parametrisation $(R, \bar{\boldsymbol{u}})$ of the Lagrangian, neither the classical Euler-Lagrange equations nor the Noether theorem are applicable directly, as a key assumption behind these equations, $\boldsymbol{q}' = \frac{\partial \boldsymbol{q}}{\partial s}$, is lost in the case of 3D rotations. This difficulty can however be overcome by imposing commutativity of derivation and perturbation operators, leading to so-called *compatibility* constraints. In the end, this method allows one to formulate Noether's theorem directly on the right spaces containing the two different types of variables, i.e. $\mathbb{R}^n$ for translational quantities (such as the rod centreline), and $\mathcal{SO}(3)$ for rotational quantities (such as the rod material frame), without the need for additional constraints to maintain the variables in their native space. For rods, one last constraint that couples translational quantities to rotational quantities still needs to be added in the Lagrangian formulation, but in practice this one remains very simple. The most painful constraints, which are the ones expressing that $\boldsymbol{q}$ is a rotation matrix, are eliminated with the second 'compact' method. In the end, we come up with simple recipes that can be used for any problem containing translational and rotational parts, possibly coupled together.

The Euler-Lagrange equations have been expressed on $\mathbb{R}^3 \times \mathcal{SO}(3)$ for a while, mainly by roboticians dealing with rigid body systems, see e.g. (Lee et al., 2018) for a good introduction to this topic and a derivation of the Euler-Lagrange equations on $\mathbb{R}^3 \times \mathcal{SO}(3)$ for dynamic rigid body systems. Romero and Gebhardt (2020) recently applied $\mathbb{R}^n \times \mathcal{SO}(3)$ Euler-Lagrange equations to derive static and dynamic equations for (extensible) Kirchhoff thin elastic rods.

To the best of our knowledge, this approach has not yet been derived to the more general Reissner assumptions nor to derive Noether's principle on $\mathbb{R}^n \times \mathcal{SO}(3)$ for thin elastic rods. In the following we summarise the main results we obtained for the Euler-Lagrange equations and Noether's theorem on $\mathbb{R}^n \times \mathcal{SO}(3)$ in the static case. We mention briefly in Sections 5 and 8 how we can apply these new Noether invariants to our static rod problems to retrieve the same results as with the 'flattening' method, in a more straightforward way. Details of the derivations are provided in Appendix A.

Arclength invariant. We consider two types of degrees of freedom: translational ones, denoted as before as $\boldsymbol{q}$, a vector of $\mathbb{R}^n$; and a rotational one[1], denoted as $R \in \mathcal{SO}(3)$, with $R' = R\,[\bar{\boldsymbol{u}}]_\times$ and $\bar{\boldsymbol{u}} \in \mathbb{R}^3$. We denote by $\mathring{\mathcal{L}}(\boldsymbol{q}, \boldsymbol{q}', R, \bar{\boldsymbol{u}})$ the Lagrangian functional that uses $\bar{\boldsymbol{u}}$ to represent the derivative of the rotation matrix R.

In the particular static case, we obtain the following invariant quantity if $\mathring{\mathcal{L}}$ does not explicitly depends on s,

$$\forall s, \quad \mathring{H}'(s) = 0 \qquad \text{with} \quad \mathring{H}(s) = \mathring{H} = \boldsymbol{q}' \cdot \frac{\partial \mathring{\mathcal{L}}}{\partial \boldsymbol{q}'} + \bar{\boldsymbol{u}} \cdot \frac{\partial \mathring{\mathcal{L}}}{\partial \bar{\boldsymbol{u}}} - \mathring{\mathcal{L}}. \tag{8}$$

[1] In case of multiple rotational degrees of freedom R_i, a similar formula applies with u being the concatenation of all vectors $\bar{\boldsymbol{u}}_i$.

Proof is given in Appendix A. Note that the rotational part of the invariant takes the same form as the translational part, with $\bar{\boldsymbol{u}}$ playing the role of R's derivative. Besides, the formula above is valid for any one-dimensional system featuring translational and/or rotational parts. As seen later, examples include statics of elastic rods, with $\bar{\boldsymbol{u}}$ being the triplet of material curvatures and twist, but also dynamic rigid bodies, with s representing time and $\bar{\boldsymbol{u}}$ corresponding to the angular velocity vector. In particular, in the case of a dynamic rigid body, H corresponds to the Hamiltonian of the system (expressed as the Legendre transform of the Lagrangian), with $\frac{\partial \mathcal{L}}{\partial \boldsymbol{q}'}$ the linear momentum and $\frac{\partial \mathcal{L}}{\partial \bar{\boldsymbol{u}}}$ the angular momentum (Lee et al., 2018, Chapter 7). If H has no explicit dependence in time (e.g. case of a freely moving rigid body), then it is well-known that H coincides with the total mechanical energy of the system, hence it is constant over time.

Configuration rotation invariant. Let $\epsilon\boldsymbol{\theta}$ a vector around which the rotation matrix R undergoes an infinitesimal rotation, i.e. we consider the transformation $\tilde{R} = R + \epsilon R\,[\boldsymbol{\theta}]_\times$. If this operation leaves the lagrangian $\mathring{\mathcal{L}}$ unchanged, then the following relation holds,

$$\left(\boldsymbol{\theta}\cdot\frac{\partial\mathring{\mathcal{L}}}{\partial\bar{\boldsymbol{u}}}\right)' = 0 \quad \forall s. \tag{9}$$

Proof is given in Appendix A. Again, note that this invariant takes the same form as the translational counterpart (4a), with $\bar{\boldsymbol{u}}$ playing the role of R's derivative.

3. Thin elastic rod problem setup

Prerequisites. Let $\boldsymbol{x}$ a vector of $\mathbb{R}^3$. In the basis $(\boldsymbol{d_1}, \boldsymbol{d_2}, \boldsymbol{d_3})$, the vector reads $\boldsymbol{x} = x_1\boldsymbol{d_1} + x_2\boldsymbol{d_2} + x_3\boldsymbol{d_3} = \sum x_i\boldsymbol{d_i}$.

We have

$$x_i' = (\boldsymbol{x}' + \boldsymbol{x}\times\boldsymbol{u})\cdot\boldsymbol{d_i} \tag{10}$$

hence

$$\boldsymbol{x}'\cdot\boldsymbol{d_i} = x_i' - (\boldsymbol{x}\times\boldsymbol{u})\cdot\boldsymbol{d_i}. \tag{11}$$

3.1. Potential energy

We consider a shearable, extensible, bendable, twistable elastic rod. The rod has a natural shape that is not necessarily straight. We use an arclength parametrisation with the variable s. We start with the internal bending and twist energy densities,

$$W_{\text{bend}} = \frac{1}{2}B_1\,(u_1(s)-\hat{u}_1)^2 + \frac{1}{2}B_2\,(u_2(s)-\hat{u}_2)^2 + \frac{1}{2}B_3\,(u_3(s)-\hat{u}_3)^2 \tag{12}$$

where the u_i are actual curvatures and twist of the rod, and the $\hat{u}_i$ their natural counterparts. We also consider the elastic energy density due to shear and stretch,

$$W_{\text{shear}} = \frac{1}{2}A_1\,(v_1(s)-\hat{v}_1)^2 + \frac{1}{2}A_2\,(v_2(s)-\hat{v}_2)^2 + \frac{1}{2}A_3\,(v_3(s)-\hat{v}_3)^2 \tag{13}$$

where the v_i are actual shear and stretch of the rod, and the $\hat{v}_i$ their natural counterparts. Generally, it is considered that $\hat{v}_1 = 0$, $\hat{v}_2 = 0$, and $\hat{v}_3 = 1$, in which case s is the arclength of the rod in the natural state, but we will at first keep generic $\hat{v}_i$ values to exhibit symmetric formulas, see e.g. (29).

We finally add the potential energy density W_{ext} associated to the external conservative force density $\boldsymbol{f}_{\text{ext}}$, i.e. $\boldsymbol{f}_{\text{ext}} = -\partial/\partial\boldsymbol{r}W_{\text{ext}}(\boldsymbol{r})$, to obtain the total potential energy density of the rod V,

$$V = W_{\text{bend}} + W_{\text{shear}} + W_{\text{ext}}. \tag{14}$$

In the case where $\boldsymbol{f}_{\text{ext}}$ is simply the gravitational force density $\boldsymbol{f}_{\text{ext}} = -\rho S\,g\,\boldsymbol{e}_z$, we have $W_{\text{ext}}(\boldsymbol{r}) = \rho S\,g\,\boldsymbol{r}(s)\cdot\boldsymbol{e}_z$, where ρ is the density of the material, S the area of the rod cross-section, and g the norm of the acceleration of gravity, see also (O'Reilly, 2015) where the weight was introduced in the invariant.

3.2. Constraints

We attach a Cosserat orthonormal frame $R(s) = (\boldsymbol{d_1}(s), \boldsymbol{d_2}(s), \boldsymbol{d_3}(s))$ – also called material frame – to the rod, which brings 6 constraints

$$\boldsymbol{d_1}\cdot\boldsymbol{d_1} - 1 = 0 \qquad \boldsymbol{d_2}\cdot\boldsymbol{d_2} - 1 = 0 \qquad \boldsymbol{d_3}\cdot\boldsymbol{d_3} - 1 = 0 \tag{15a}$$

$$\boldsymbol{d_1}\cdot\boldsymbol{d_2} = 0 \qquad \boldsymbol{d_2}\cdot\boldsymbol{d_3} = 0 \qquad \boldsymbol{d_3}\cdot\boldsymbol{d_1} = 0 \tag{15b}$$

The conservation of these orthonormal relations as s is varied along the rod implies the Darboux relation

$$\boldsymbol{d}_1'(s) = \boldsymbol{u}\times\boldsymbol{d_1} \tag{16a}$$

$$\boldsymbol{d}_2'(s) = \boldsymbol{u}\times\boldsymbol{d_2} \tag{16b}$$

$$\boldsymbol{d}_3'(s) = \boldsymbol{u}\times\boldsymbol{d_3} \tag{16c}$$

where the Darboux vector has been chosen to be $\boldsymbol{u} = u_1\boldsymbol{d_1} + u_2\boldsymbol{d_2} + u_3\boldsymbol{d_3}$, see e.g. (Antman, 2004). The three vectorial relations (16) are constraints for the three scalar components u_1, u_2, u_3 and can thereof be rewritten as

$$u_1 = \boldsymbol{d}_2'\cdot\boldsymbol{d_3}\,, \quad u_2 = \boldsymbol{d}_3'\cdot\boldsymbol{d_1}\,, \quad u_3 = \boldsymbol{d}_1'\cdot\boldsymbol{d_2} \tag{17}$$

The rod centreline $\boldsymbol{r}(s)$ is linked to the Cosserat frame through the relation

$$\boldsymbol{r}'(s) = \boldsymbol{v}(s) = v_1(s)\,\boldsymbol{d_1} + v_2(s)\,\boldsymbol{d_2} + v_3(s)\,\boldsymbol{d_3}. \tag{18}$$

4. Thin elastic rod equations from the Lagrangian

We seek equilibrium states for this elastic rod by minimizing its total potential energy V. We only consider the necessary conditions for the vanishing of the first variation of V under the continuous constraints (15), (17), and (18).

4.1. Lagrangian

Using the Lagrange multiplier rule, we introduce the Lagrangian on $\mathbb{R}^n$,

$$\begin{aligned}\mathcal{L} = V &+ \boldsymbol{\lambda_r}\cdot(\boldsymbol{r}'(s) - v_1(s)\,\boldsymbol{d_1} - v_2(s)\,\boldsymbol{d_2} - v_3(s)\,\boldsymbol{d_3}) + \lambda_{u_1}\left(\boldsymbol{d}_2'\cdot\boldsymbol{d_3} - u_1\right) + \lambda_{u_2}\left(\boldsymbol{d}_3'\cdot\boldsymbol{d_1} - u_2\right) + \lambda_{u_3}\left(\boldsymbol{d}_1'\cdot\boldsymbol{d_2} - u_3\right)\\ &+ \lambda_{11}\,\frac{1}{2}\,(1 - \boldsymbol{d_1}\cdot\boldsymbol{d_1}) + \lambda_{22}\,\frac{1}{2}\,(1 - \boldsymbol{d_2}\cdot\boldsymbol{d_2}) + \lambda_{33}\,\frac{1}{2}\,(1 - \boldsymbol{d_3}\cdot\boldsymbol{d_3})\\ &+ \lambda_{12}\,\boldsymbol{d_1}\cdot\boldsymbol{d_2} + \lambda_{23}\,\boldsymbol{d_2}\cdot\boldsymbol{d_3} + \lambda_{31}\,\boldsymbol{d_3}\cdot\boldsymbol{d_1}\end{aligned} \tag{19}$$

where $\mathcal{L} = \mathcal{L}[\boldsymbol{q}(s), \boldsymbol{q}'(s)]$ with $\boldsymbol{q} = (\boldsymbol{r}, \boldsymbol{d_1}, \boldsymbol{d_2}, \boldsymbol{d_3}, u_1, u_2, u_3, v_1, v_2, v_3)$, see also (Elettro et al., 2017) for a similar approache in the context of elasto-capillarity.

Alternatively, we can choose to parameterise the derivative of the Cosserat frame $R(s)$, which belongs to $\mathcal{SO}(3)$, using the Darboux vector $\boldsymbol{u}$, such that $R'(s) = [\boldsymbol{u}]_\times R = R\,[\bar{\boldsymbol{u}}]_\times$. The vector $\bar{\boldsymbol{u}}$ is the triplet containing the material curvatures and twist u_i, i.e. we have $\boldsymbol{u} = R\,\bar{\boldsymbol{u}}$. In this case, our new Lagrangian $\mathring{\mathcal{L}} = \mathring{\mathcal{L}}[\boldsymbol{q}, R, \boldsymbol{q}', \bar{\boldsymbol{u}}]$ on $\mathbb{R}^n \times \mathcal{SO}(3)$ simply reads

$$\begin{aligned}\mathring{\mathcal{L}} &= V + \boldsymbol{\lambda_r}\cdot(\boldsymbol{r}'(s) - v_1(s)\,\boldsymbol{d_1} - v_2(s)\,\boldsymbol{d_2} - v_3(s)\,\boldsymbol{d_3})\\ &= V + \boldsymbol{\lambda_r}\cdot(\boldsymbol{r}'(s) - R(s)\,\boldsymbol{v}(s))\,,\end{aligned} \tag{20}$$

as the constraints for maintaining $R(s)$ in $\mathcal{SO}(3)$ are now intrinsically accounted for thanks to our $\mathcal{SO}(3)$ parameterisation $(R, \bar{\boldsymbol{u}})$ of the material frame. Only the constraints relating the material frame $R(s)$ to the centreline $\boldsymbol{r}'(s)$ of the rod remains.

4.2. Euler-Lagrange equations

From the Lagrangian on $\mathbb{R}^n$. Necessary conditions for the vanishing of the first variation of V are the classical Euler-Lagrange equations

$$\frac{\partial \mathcal{L}}{\partial \boldsymbol{r}} = \left(\frac{\partial \mathcal{L}}{\partial \boldsymbol{r}'}\right)' \Rightarrow \boldsymbol{\lambda}_{\boldsymbol{r}}'(s) = -\boldsymbol{f}_{\text{ext}} \tag{21a}$$

$$\frac{\partial \mathcal{L}}{\partial u_1} = 0 \Rightarrow \lambda_{u_1} = B_1(u_1 - \hat{u}_1) \tag{21b}$$

$$\frac{\partial \mathcal{L}}{\partial u_2} = 0 \Rightarrow \lambda_{u_2} = B_2(u_2 - \hat{u}_2) \tag{21c}$$

$$\frac{\partial \mathcal{L}}{\partial u_3} = 0 \Rightarrow \lambda_{u_3} = B_3(u_3 - \hat{u}_3) \tag{21d}$$

$$\frac{\partial \mathcal{L}}{\partial v_1} = 0 \Rightarrow \boldsymbol{\lambda}_{\boldsymbol{r}} \cdot \boldsymbol{d}_1 = A_1(v_1 - \hat{v}_1) \tag{21e}$$

$$\frac{\partial \mathcal{L}}{\partial v_2} = 0 \Rightarrow \boldsymbol{\lambda}_{\boldsymbol{r}} \cdot \boldsymbol{d}_2 = A_2(v_2 - \hat{v}_2) \tag{21f}$$

$$\frac{\partial \mathcal{L}}{\partial v_3} = 0 \Rightarrow \boldsymbol{\lambda}_{\boldsymbol{r}} \cdot \boldsymbol{d}_3 = A_3(v_3 - \hat{v}_3) \tag{21g}$$

$$\frac{\partial \mathcal{L}}{\partial \boldsymbol{d_1}} = \left(\frac{\partial \mathcal{L}}{\partial \boldsymbol{d}_1'}\right)' \Rightarrow \lambda_{u_3} \boldsymbol{d}_2' - \lambda_{u_2} \boldsymbol{d}_3' + \lambda_{u_3}' \boldsymbol{d_2} + \boldsymbol{\lambda}_{\boldsymbol{r}} v_1 + \lambda_{11} \boldsymbol{d_1} - \lambda_{12} \boldsymbol{d_2} - \lambda_{31} \boldsymbol{d_3} = 0 \tag{21h}$$

$$\frac{\partial \mathcal{L}}{\partial \boldsymbol{d_2}} = \left(\frac{\partial \mathcal{L}}{\partial \boldsymbol{d}_2'}\right)' \Rightarrow \lambda_{u_1} \boldsymbol{d}_3' - \lambda_{u_3} \boldsymbol{d}_1' + \lambda_{u_1}' \boldsymbol{d_3} + \boldsymbol{\lambda}_{\boldsymbol{r}} v_2 + \lambda_{22} \boldsymbol{d_2} - \lambda_{23} \boldsymbol{d_3} - \lambda_{12} \boldsymbol{d_1} = 0 \tag{21i}$$

$$\frac{\partial \mathcal{L}}{\partial \boldsymbol{d_3}} = \left(\frac{\partial \mathcal{L}}{\partial \boldsymbol{d}_3'}\right)' \Rightarrow \lambda_{u_2} \boldsymbol{d}_1' - \lambda_{u_1} \boldsymbol{d}_2' + \lambda_{u_2}' \boldsymbol{d_1} + \boldsymbol{\lambda}_{\boldsymbol{r}} v_3 + \lambda_{33} \boldsymbol{d_3} - \lambda_{31} \boldsymbol{d_1} - \lambda_{23} \boldsymbol{d_2} = 0. \tag{21j}$$

We recognise in (21a) the force balance of the static Reissner equations, with the Lagrange multiplier $\boldsymbol{\lambda}_{\boldsymbol{r}}$ playing the role of the internal force vector $\boldsymbol{n} = \boldsymbol{\lambda}_{\boldsymbol{r}}$. We also identify in (21b) – (21d) the bend-twist constitutive relations, where the Lagrange multipliers λ_{u_i} are the components in the material frame of the internal moment vector $\boldsymbol{m} = \lambda_{u_1} \boldsymbol{d_1} + \lambda_{u_2} \boldsymbol{d_2} + \lambda_{u_3} \boldsymbol{d_3}$, and finally in (21e) – (21g) the shear-extension constitutive relations which provide the components in the material frame of the internal force vector $\boldsymbol{n} = \boldsymbol{\lambda}_{\boldsymbol{r}}$.

The Euler-Lagrange equations related to $\boldsymbol{d_1}, \boldsymbol{d_2}, \boldsymbol{d_3}$ require more manipulations. By taking the scalar product of (21i), (21j), (21h) with, respectively $\boldsymbol{d_3}$, $\boldsymbol{d_1}$, $\boldsymbol{d_2}$, we obtain the moment balance of the static Reissner equations,

$$m_1'(s) = \lambda_{23} - v_2\, n_3 - u_2\, m_3 \tag{22a}$$

$$m_2'(s) = \lambda_{31} - v_3\, n_1 - u_3\, m_1 \tag{22b}$$

$$m_3'(s) = \lambda_{12} - v_1\, n_2 - u_1\, m_2 \tag{22c}$$

with the notation $\boldsymbol{n} = n_1\, \boldsymbol{d_1} + n_2\, \boldsymbol{d_2} + n_3\, \boldsymbol{d_3}$. To compute the missing multipliers $\lambda_{23}, \lambda_{31}, \lambda_{12}$, we take the scalar product of (21j), (21h), (21i) with, respectively $\boldsymbol{d_2}$, $\boldsymbol{d_3}$, $\boldsymbol{d_1}$

$$\lambda_{23} = \lambda_{u_2}\, u_3 + n_2\, v_3 \tag{23a}$$

$$\lambda_{31} = \lambda_{u_3}\, u_1 + n_3\, v_1 \tag{23b}$$

$$\lambda_{12} = \lambda_{u_1}\, u_2 + n_1\, v_2 \tag{23c}$$

We inject (23) into (22) to obtain:

$$m_1'(s) = u_3 m_2 - u_2 m_3 + v_3 n_2 - v_2 n_3 \tag{24a}$$

$$m_2'(s) = u_1 m_3 - u_3 m_1 + v_1 n_3 - v_3 n_1 \tag{24b}$$

$$m_3'(s) = u_2 m_1 - u_1 m_2 + v_2 n_1 - v_1 n_2 \tag{24c}$$

and using (11) we finally arrive at

$$m'(s) = n(s) \times r'(s) \tag{25}$$

The force equilibrium expressed in the material frame reads

$$n_1'(s) = u_3 n_2 - u_2 n_3 - f_{\text{ext}} \cdot d_1 \tag{26a}$$
$$n_2'(s) = u_1 n_3 - u_3 n_1 - f_{\text{ext}} \cdot d_2 \tag{26b}$$
$$n_3'(s) = u_2 n_1 - u_1 n_2 - f_{\text{ext}} \cdot d_3 \tag{26c}$$

From the Lagrangian on $\mathbb{R}^n \times \mathcal{SO}(3)$. The method above has the advantage to be simple and explicit, since all computations are led on $\mathbb{R}^n$ using standard Euler-Lagrange equations. However, on may argue that computing $\frac{\partial \mathcal{L}}{\partial d'_{123}}$ (21h, 21i, and 21j) may be lengthy, and overall refactoring all terms to recover rod equations is a bit tedious.

In contrast, starting from the reduced Lagrangian $\mathring{\mathcal{L}}$ given in (20) and using the Euler-Lagrange equations (A.7) on $\mathbb{R}^n \times \mathcal{SO}(3)$ alleviates most of these computations, see Appendix A. Again, we see that the internal force $\boldsymbol{n}$ emerges as the Lagrange multiplier associated to the constraint relating the material frame to the centreline of the rod. In contrast, the internal moment $\boldsymbol{m}$ no longer appears as a multiplier, but directly stems from the term $\frac{\partial \mathring{\mathcal{L}}}{\partial \bar{u}}$ owing to the reduced parametrisation of $\mathcal{SO}(3)$.

5. Noether invariants in the static case

5.1. Arclength translation

From the Lagrangian on $\mathbb{R}^n$. As the Lagrangian does not explicitly depend on s, the following quantity is, at equilibrium and under satisfied constraints, uniform along the rod, see (4b)

$$H'(s) = 0 \text{ with } H = \frac{\partial \mathcal{L}}{\partial \boldsymbol{q}'} \cdot \boldsymbol{q}' - \mathcal{L}. \tag{27}$$

with $\boldsymbol{q} = (\boldsymbol{r}, \boldsymbol{d_1}, \boldsymbol{d_2}, \boldsymbol{d_3}, u_1, u_2, u_3, v_1, v_2, v_3)$. The notation H seems natural when one considers that the relation (27) is closely linked to the Legendre transformation of the Lagrangian $\mathcal{L}$. The quantity H is invariant for an equilibrium solution, that is, when the constraints (15), (17), and (18) are satisfied. In this case $\mathcal{L} = V$ and

$$\frac{\partial \mathcal{L}}{\partial \boldsymbol{q}'} \cdot \boldsymbol{q}' = \boldsymbol{n} \cdot \boldsymbol{r}' + m_3\, \boldsymbol{d_2} \cdot \boldsymbol{d}_1' + m_1\, \boldsymbol{d_3} \cdot \boldsymbol{d}_2' + m_2\, \boldsymbol{d_1} \cdot \boldsymbol{d}_3' \tag{28a}$$
$$= \boldsymbol{n} \cdot \boldsymbol{v} + \boldsymbol{m} \cdot \boldsymbol{u}, \tag{28b}$$

which gives

$$H = \boldsymbol{n} \cdot \boldsymbol{v} + \boldsymbol{m} \cdot \boldsymbol{u} - V. \tag{29}$$

From the Lagrangian on $\mathbb{R}^n \times \mathcal{SO}(3)$. Using our compact Lagrangian (20) and the Noether invariant (8) derived on $\mathbb{R}^n \times \mathcal{SO}(3)$ (see Appendix A), we immediately recover the same invariant $\mathring{H} = H$, as $\frac{\partial \mathring{\mathcal{L}}}{\partial \boldsymbol{r}'}$ stands for the internal force $\boldsymbol{n}$ and $\frac{\partial \mathring{\mathcal{L}}}{\partial \bar{u}}$ for the internal moment $\boldsymbol{m}$.

Interpretation of H. Using (14), the mixed (strain-stress) formulation (29) can be rewritten in different ways,

$$H = \frac{1}{2}\boldsymbol{m} \cdot (\boldsymbol{u} + \hat{\boldsymbol{u}}) + \frac{1}{2}\boldsymbol{n} \cdot (\boldsymbol{v} + \hat{\boldsymbol{v}}) - W_{\text{ext}} \tag{30a}$$
$$H = W_{\text{bend}} + \boldsymbol{m} \cdot \hat{\boldsymbol{u}} + W_{\text{shear}} + \boldsymbol{n} \cdot \hat{\boldsymbol{v}} - W_{\text{ext}} \tag{30b}$$
$$H = \frac{1}{2}B_i(u_i^2 - \hat{u}_i^2) + \frac{1}{2}A_i(v_i^2 - \hat{v}_i^2) - W_{\text{ext}}, \tag{30c}$$

Starting from (30b), we obtain in the classical Reissner case ($\hat{v}_1 = \hat{v}_2 = 0$ and $\hat{v}_3 = 1$, and any value for $\hat{\boldsymbol{u}}$)

$$H = W_{\text{bend}} + \boldsymbol{m} \cdot \hat{\boldsymbol{u}} + W_{\text{shear}} + n_3 - W_{\text{ext}} = \frac{1}{2}B_i(u_i^2 - \hat{u}_i^2) + W_{\text{shear}} + n_3 - W_{\text{ext}}, \tag{31}$$

Note that the emergence in the formula of the third component of the internal force $\boldsymbol{n}$, the tension n_3, simply stems from the (standard) choice to parametrise the natural shape of the rod with its rest arclength s, i.e. $\hat{v}_1 = \hat{v}_2 = 0$, and $\hat{v}_3 = 1$. In the further particular case where all the natural strains vanish ($\hat{u}_1 = \hat{u}_2 = \hat{u}_3 = \hat{v}_1 = \hat{v}_2 = 0$ and $\hat{v}_3 = 1$), a formulation with energies is obtained

$$H = W_{\text{bend}} + W_{\text{shear}} + n_3 - W_{\text{ext}}. \tag{32}$$

Finally, in the absence of any external force $W_{\text{ext}} = 0$ and in the inextensible, unshearable case (inextensible Kirchhoff), where $W_{\text{shear}} = 0$, we re-obtain the Hamiltonian used in (Kehrbaum and Maddocks, 1997),

$$H = \frac{1}{2}\boldsymbol{m}\cdot(\boldsymbol{u} + \hat{\boldsymbol{u}}) + n_3. \tag{33}$$

Generalisation: hyperelastic rods and ribbons. It should be remarked that the invariant H is not restricted to the quadratic energy (12) but also stands for hyperlastic rods (Maddocks and Dichmann, 1994; O'Reilly, 2017). Moreover, 1D models of elastic ribbons also fall into the realm of application of the invariant, see for example (Starostin and van der Heijden, 2015; Borum, 2018; Neukirch and Audoly, 2021). See also (Audoly and van der Heijden, 2022) and (Charrondière et al., 2024) for an example of how the invariant may be used in boundary layer calculations in the case of the Wunderlich strain energy. We here give the example of an inextensible, unshearable, Sadowsky ribbon (Dias and Audoly, 2015; Charrondière et al., 2020) with uniform natural curvature $\hat{u}_1$

$$W^{sdw}_{bend} = \frac{1}{2}B^{\star}\left[u_1^2\left(1 + \frac{u_3^2}{u_1^2}\right)^2 - 2\hat{u}_1\, u_1\left(1 + \nu\frac{u_3^2}{u_1^2}\right)\right] \tag{34a}$$

$$W^{sdw}_{shear} = 0 \tag{34b}$$

where ν is the Poisson ratio of the elastic material, $u_2 = 0$, and $B^{\star} = B/(1+\nu^2)$. In this case, the invariant H (29) interestingly does not depend on the natural curvature $\hat{u}_1$

$$H^{sdw} = \boldsymbol{n}\cdot\boldsymbol{v} + \boldsymbol{m}\cdot\boldsymbol{u} - V = n_3 + \boldsymbol{m}\cdot\boldsymbol{u} - W^{sdw}_{bend} - W_{ext} = n_3 + \frac{1}{2}B^{\star}u_1^2\left(1 + \frac{u_3^2}{u_1^2}\right)^2 - W_{ext} \tag{35a}$$

whereas in the case for rods with natural curvature, see (33), the dependance is present.

5.2. Configuration translation

In the absence of any external force field, $W_{\text{ext}} = 0$, if we consider the transformation $\tilde{\boldsymbol{r}} = \boldsymbol{r} + \boldsymbol{a}$, which is a translation of the position by a fixed amount $\boldsymbol{a}$, the Lagrangian (19) stays the same:

$$\tilde{\boldsymbol{r}} = \boldsymbol{r} + \boldsymbol{a} \quad \Rightarrow \quad \mathcal{L}(\tilde{\boldsymbol{r}}, \boldsymbol{d_1}, \boldsymbol{d_2}, \boldsymbol{d_3}, u_1, u_2, u_3, v_1, v_2, v_3) = \mathcal{L}(\boldsymbol{r}, \boldsymbol{d_1}, \boldsymbol{d_2}, \boldsymbol{d_3}, u_1, u_2, u_3, v_1, v_2, v_3) \tag{36}$$

In this case, $\boldsymbol{\theta}$ in (4a) is in fact the vector $\boldsymbol{a}$ and the invariant is

$$\left[\boldsymbol{a}\cdot\frac{\partial\mathcal{L}}{\partial\boldsymbol{r}'}\right]' = 0 \quad \forall\boldsymbol{a} \quad \Rightarrow \quad \boldsymbol{n}' = 0 \tag{37}$$

We see that the force vector is uniform along the rod if no external force field is applied to the rod, a classical result which is readily included in (21a).

5.3. Configuration rotation

In the absence of any external force field, $W_{\text{ext}} = 0$, we further consider the transformation where the configuration $(\boldsymbol{r}, \boldsymbol{d_1}, \boldsymbol{d_2}, \boldsymbol{d_3})$ is rotated by a small angle ϵ around an arbitrary, constant, vector $\boldsymbol{b}$. The transformation reads

$$\tilde{\boldsymbol{r}} = \boldsymbol{r} + \epsilon\,\boldsymbol{b}\times\boldsymbol{r}\,, \quad \tilde{\boldsymbol{d}}_{1,2,3} = \boldsymbol{d_{1,2,3}} + \epsilon\,\boldsymbol{b}\times\boldsymbol{d_{1,2,3}}\,. \tag{38}$$

Note that the vectors $\boldsymbol{v}$ and $\boldsymbol{u}$ are also rotated, but their components $v_{1,2,3}$ and $u_{1,2,3}$ stay unchanged. Standard Taylor expansion shows that, at leading ordre in ϵ, this transformation leaves the Lagrangian invariant

$$\mathcal{L}(\tilde{\boldsymbol{r}}, \tilde{\boldsymbol{d}}_1, \tilde{\boldsymbol{d}}_2, \tilde{\boldsymbol{d}}_3, u_1, u_2, u_3, v_1, v_2, v_3) = \mathcal{L}(\boldsymbol{r}, \boldsymbol{d_1}, \boldsymbol{d_2}, \boldsymbol{d_3}, u_1, u_2, u_3, v_1, v_2, v_3) \tag{39}$$

and consequently, the following quantity is invariant

$$\left[\boldsymbol{b} \times \boldsymbol{r} \cdot \frac{\partial \mathcal{L}}{\partial \boldsymbol{r}'} + \boldsymbol{b} \times \boldsymbol{d}_{1,2,3} \cdot \frac{\partial \mathcal{L}}{\partial \boldsymbol{d}'_{1,2,3}} \right]' = 0 \tag{40a}$$

$$[\boldsymbol{b} \cdot \boldsymbol{r}(s) \times \boldsymbol{n} + \boldsymbol{b} \cdot \boldsymbol{m}(s)]' = 0 \quad \forall \boldsymbol{b} \tag{40b}$$

$$[\boldsymbol{r}(s) \times \boldsymbol{n} + \boldsymbol{m}(s)]' = 0 \tag{40c}$$

As the configuration translation, the rotation invariant is just the moment equilibrium (25).

5.4. *Configuration rotation around the fixed force axis*

In the absence of any external force field, $W_{\text{ext}} = 0$, section (5.2) showed the force vector $\boldsymbol{n}$ is a fixed quantity. In this case, we consider the transformation in which the vectors $\boldsymbol{r}$, $\boldsymbol{d_1}$, $\boldsymbol{d_2}$, and $\boldsymbol{d_3}$ are rotated by a small angle ϵ around the force axis $\boldsymbol{n}$

$$\tilde{\boldsymbol{r}} = \boldsymbol{r} + \epsilon\, \boldsymbol{n} \times \boldsymbol{r}\,, \quad \tilde{\boldsymbol{d}}_{1,2,3} = \boldsymbol{d}_{1,2,3} + \epsilon\, \boldsymbol{n} \times \boldsymbol{d}_{1,2,3}\,. \tag{41}$$

Note that the vectors $\boldsymbol{v}$ and $\boldsymbol{u}$ are also rotated, but their components $v_{1,2,3}$ and $u_{1,2,3}$ stay unchanged. At leading ordre in ϵ, this transformation leaves the Lagrangian invariant

$$\mathcal{L}(\tilde{\boldsymbol{r}}, \tilde{\boldsymbol{d}}_1, \tilde{\boldsymbol{d}}_2, \tilde{\boldsymbol{d}}_3, u_1, u_2, u_3, v_1, v_2, v_3) = \mathcal{L}(\boldsymbol{r}, \boldsymbol{d}_1, \boldsymbol{d}_2, \boldsymbol{d}_3, u_1, u_2, u_3, v_1, v_2, v_3) \tag{42}$$

and consequently, the following quantity is invariant

$$\left[\boldsymbol{n} \times \boldsymbol{r} \cdot \frac{\partial \mathcal{L}}{\partial \boldsymbol{r}'} + \boldsymbol{n} \times \boldsymbol{d}_{1,2,3} \cdot \frac{\partial \mathcal{L}}{\partial \boldsymbol{d}'_{1,2,3}} \right]' = 0 \tag{43}$$

$$[\boldsymbol{n} \cdot \boldsymbol{m}(s)]' = 0 \tag{44}$$

5.5. *Configuration rotation around the section normal*

In the presence or absence of an external force field, we now consider the transformation where the vectors $\boldsymbol{d_1}$, $\boldsymbol{d_2}$ are rotated by a small angle ϵ around the vector $\boldsymbol{d_3}$. In addition, the (1,2) components of the vectors $\boldsymbol{u}$ and $\boldsymbol{v}$ are transformed as well so as to leave the vectors $\boldsymbol{u}$ and $\boldsymbol{v}$ unchanged. The full transformation reads

$$\tilde{\boldsymbol{d}}_1 = \boldsymbol{d}_1 + \epsilon\, \boldsymbol{d}_3 \times \boldsymbol{d}_1\,, \quad \tilde{\boldsymbol{d}}_2 = \boldsymbol{d}_2 + \epsilon\, \boldsymbol{d}_3 \times \boldsymbol{d}_2\,, \quad \tilde{u}_1 = u_1 + \epsilon\, u_2\,, \quad \tilde{u}_2 = u_2 - \epsilon\, u_1\,, \quad \tilde{v}_1 = v_1 + \epsilon\, v_2\,, \quad \tilde{v}_2 = v_2 - \epsilon\, v_1\,, \tag{45}$$

In the case where $A_1 = A_2$, $B_1 = B_2$, $\hat{u}_1 = 0$, $\hat{u}_2 = 0$, $\hat{v}_1 = 0$, and $\hat{v}_2 = 0$, at leading ordre in ϵ, this transformation leaves the Lagrangian invariant

$$\mathcal{L}(\tilde{\boldsymbol{r}}, \tilde{\boldsymbol{d}}_1, \tilde{\boldsymbol{d}}_2, \boldsymbol{d}_3, \tilde{u}_1, \tilde{u}_2, u_3, \tilde{v}_1, \tilde{v}_2, v_3) = \mathcal{L}(\boldsymbol{r}, \boldsymbol{d}_1, \boldsymbol{d}_2, \boldsymbol{d}_3, u_1, u_2, u_3, v_1, v_2, v_3) \tag{46}$$

and consequently, the following quantity is invariant

$$\left[\boldsymbol{d}_3 \times \boldsymbol{d}_1 \cdot \frac{\partial \mathcal{L}}{\partial \boldsymbol{d}'_1} + \boldsymbol{d}_3 \times \boldsymbol{d}_2 \cdot \frac{\partial \mathcal{L}}{\partial \boldsymbol{d}'_2} + u_2 \frac{\partial \mathcal{L}}{\partial u'_1} - u_1 \frac{\partial \mathcal{L}}{\partial u'_2} + v_2 \frac{\partial \mathcal{L}}{\partial v'_1} - v_1 \frac{\partial \mathcal{L}}{\partial v'_2} \right]' = 0 \tag{47}$$

$$[m_3(s)]' = 0 \tag{48}$$

Please note that this result holds in the case where $\hat{u}_3 \neq 0$ and $\hat{v}_3 \neq 0$.

Remarkably, one can immediately recover all the invariant properties above by using the Noether's configuration rotation formula (9) derived on $\mathcal{SO}(3)$. Using this compact formulation, two advantages are worth mentioning. First, examining the compact Lagrangian $\mathring{\mathcal{L}}$ given in (20) makes it easier to localise symmetries. Second, it is remarkable that all Noether configuration invariants for rods should be of the form $\boldsymbol{a} + \boldsymbol{\theta} \cdot \boldsymbol{m}$ with $\boldsymbol{a}, \boldsymbol{\theta} \in \mathbb{R}^3$.

6. Contact

6.1. Preamble: General case of shear forces

It is noteworthy that the arclength invariant H can be retrieved exactly by projecting the rod angular equilibrium equation (25) onto the Darboux vector $\boldsymbol{u}$. Now, let $\boldsymbol{f}$ be an external force applied onto the rod. The contribution of $\boldsymbol{f}$ to this projection reads $\boldsymbol{r}' \cdot \boldsymbol{f}$, leading to the equation $\frac{\mathrm{d}H}{\mathrm{d}s}(s) + \boldsymbol{r}'(s) \cdot \boldsymbol{f}(s) = 0 \quad \forall s$. If one assumes that $\boldsymbol{f}$ is a shear force, i.e. a force normal to the tangent $\boldsymbol{r}'$ of the rod at each point s of the centreline (the force can be zero), then this contribution vanishes. Hence, the Noether invariant H remains unchanged in the presence of shear forces.

We now examine the specific case of frictionless contact forces, first in the case when they are modelled using a soft potential, then when they are represented with unilateral constraints.

6.2. Contact potential and shear contact force

We assume that the system is subject to a conservative external force density $\boldsymbol{f}_{\text{ext}} = -\partial/\partial \boldsymbol{r} W_{\text{ext}}(\boldsymbol{r})$. We have seen previously that accounting for this external force amounts to adding $-W_{\text{ext}}(\boldsymbol{r})$ to the invariant H.

We can write down the contribution of this potential to H',

$$\frac{\mathrm{d}}{\mathrm{d}s}\left(-W_{\text{ext}}(\boldsymbol{r})\right) = -\boldsymbol{r}' \cdot -\partial/\partial \boldsymbol{r} W_{\text{ext}}(\boldsymbol{r}) \tag{49}$$

$$= \boldsymbol{r}' \cdot \boldsymbol{f}_{\text{ext}}, \tag{50}$$

which automatically cancels out if $\boldsymbol{f}_{\text{ext}}$ is normal to the centreline. As a result, an external conservative field W_{ext} yielding a force always normal to the centerline does not have to be included in the formula for H. Now the question is: can we find such potentials, i.e. yielding forces normal to $\boldsymbol{r}'$?

In section 7.7 we actually show that *soft potentials*, typically used for modelling contact, do *not* generate perfectly normal forces. As a result, such potentials need to be accounted for in the invariant H. Still, when they are rigidified, their corresponding force becomes orthogonal to $\boldsymbol{r}'$. In this latter case, no additional term needs to be added to the invariant H. This can be directly seen by modelling contact as a hard constraint, and this is what we show below.

6.3. Contact as a hard constraint: no contribution to H!

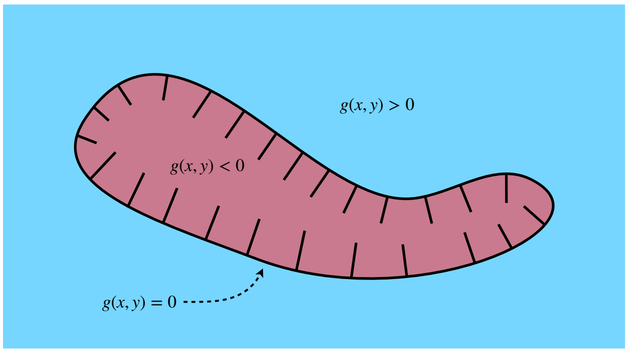

Figure 1: Contact with an obstacle in the plane may in some cases be modelled with a gap or level set function $g(x, y)$. The forbidden region has $g(x, y) < 0$, and the rod is permitted to lie in the region $g(x, y) \geq 0$. The surface of the obstacle has $g(x, y) = 0$, while $g(x, y) > 0$ in the absence of contact with the obstacle.

An interesting result emerges in the case of contact modelled as a hard constraint: there is no need to add any potential to the invariant H. Modelling contact as a hard constraint means defining a contact force using a Lagrange multiplier which acts in a normal direction compared to the rod. We already proved that a normal force yields no contribution to H. Now we prove this result again, by considering a variational point of view of the problem.

We consider a rod with centreline $\boldsymbol{r}(s)$, and an external object. We call $g(s, p)$ the gap function between $\boldsymbol{r}(s)$ and the obstacle. The gap function $g(s, p)$ might depend on parameters p of the problem that we will specify a bit later. Frictionless contact between the rod and the obstacle can be modelled by an inequality constraint of the form

$g(s,p) \geq 0\,,\ \forall s$, which expresses the fact that the two objects can be separated ($g(s,p) > 0$) or can touch each other ($g(s,p) = 0$), but are not allowed to interpenetrate, i.e. $g(s,p) < 0$ is forbidden (see figure 1). To allow this constraint to be satisfied, a Lagrange multiplier $\mu(s)$ is introduced. Mechanically, this multiplier exactly acts as a contact force that prevents the two objects from interpenetrating. Mathematically, the constraint is satisfied when the following complementarity constraint holds,

$$0 \leq g(s,p) \perp \mu(s) \geq 0,$$

which expresses that both the gap and the contact force should be non-negative, and that one has to vanish if the other one becomes positive. Intuitively, when the two objects come to contact ($g(s,p) = 0$), a contact force $\mu(s)$ gets activated. The condition above, together with the Euler-Lagrange equations actually correspond to the optimality conditions of our new variational problem, i.e. the stationarity of the action under the contact inequality constraint.

If we now go back to this initial variational view, incorporating this new inequality constraint to come up to a constraint-free problem can be done by simply modifying the Lagrangian with the additional term $\mathcal{L}_c = -\mu(s)\, g(s,p)$. As for the bilateral constraint examined in section 2, Noether's formula for the arclength invariant (5) remains valid thanks to the complementarity condition above.

Now, the point is to formulate the gap function $g(s,p)$ and examine its dependencies upon of our variables of interest, and then derive our Noether invariants. We first examine an elementary 2D case, for the sake of simplicity. We consider a 2D rod subject to contact with an infinite ground of height $y = a$. The contact inequality constraint simply reads $g(s) \geq 0$ with $g(\boldsymbol{r}) = \boldsymbol{r} \cdot \boldsymbol{e}_{\mathrm{y}} - a$, and the contribution to the Lagrangian reads $\mathcal{L}_c(\boldsymbol{r}) = -\mu(s)\,\left(\boldsymbol{r} \cdot \boldsymbol{e}_{\mathrm{y}} - a\right)$. Note that similarly to the bilaterial case, the new Lagrangian $\mathcal{L}_c$ does not contribute the $-\mathcal{L}$ part of Noether's invariant, as $\mu\, g = 0$ at equilibrium. As the contact constraint does not depend on $\boldsymbol{r}'$, it does not contribute the $\frac{\partial \mathcal{L}}{\partial \boldsymbol{r}'} \cdot \boldsymbol{r}'$ part of Noether's invariant either. Finally, such a contact constraint has no impact on the invariant. This result generalises to any gap function that depends only on $\boldsymbol{r}$.

7. Examples of applications

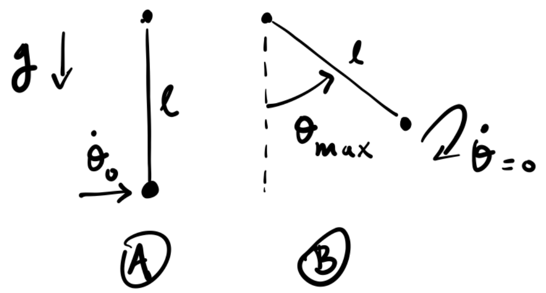

Figure 2: A pendulum, initially in its vertical equilibrium, is launched at t_A with an initial angular speed $\dot{\theta}_0$. At $t = t_B$, it will reach a maximum angle θ_{max} and start to swing back.

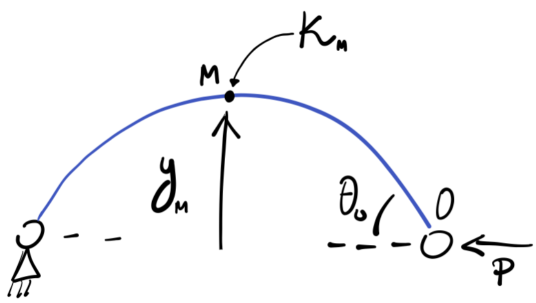

Figure 3: A planar Elastica is held with simple supports. The horizontal compressive force at the support P is yielding an equilibrium configuration with deflection θ_0, maximum vertical displacement y_M, and maximum curvature κ_M.

In this section, we illustrate several possible uses of the arclength-translation invariant (27) on the classical planar Elastica case. We consider the equilibrium of an inextensible, unshearable, naturally flat rod bent in the (x,y) plane. In this situation, twist uniformly vanishes and the Cosserat directors are such that $\boldsymbol{d_1} = -\sin\theta\, \boldsymbol{e}_{\mathrm{x}} + \cos\theta\, \boldsymbol{e}_{\mathrm{y}}$, $\boldsymbol{d_2} = \boldsymbol{e}_{\mathrm{z}}$, $\boldsymbol{d_3} = \cos\theta\, \boldsymbol{e}_{\mathrm{x}} + \sin\theta\, \boldsymbol{e}_{\mathrm{y}}$, with θ is the angle marking the deflection of the Elastica with the horizontal $\boldsymbol{e}_{\mathrm{x}}$ axis. The static Lagrangian (19) reduces to

$$\mathcal{L}(x,y,\theta,\kappa) = \frac{1}{2}\, EI\, \kappa(s)^2 + n_x(s)\,(x' - \cos\theta) + n_y(s)\,(y' - \sin\theta) + m(s)\,(\theta' - \kappa) \tag{51}$$

where we have directly used the notation for the force and moment multipliers, with $\boldsymbol{m} = m(s)\, \boldsymbol{e}_{\mathrm{y}}$. Please also note that at equilibrium, we have $n_x'(s) = 0$ and $n_y'(s) = 0$. The Euler-Lagrange equations corresponding to the variation with κ and θ lead to

$$EI\,\theta''(s) = n_x \sin\theta - n_y \cos\theta \tag{52}$$

Additionnaly, the arclength-translation invariant (33) takes the simple form

$$H = \frac{1}{2} EI\,\kappa^2 + n_3 \tag{53}$$

where $n_3 = \boldsymbol{n}\cdot\boldsymbol{d_3} = n_x \cos\theta + n_y \sin\theta$ is called the internal tension in the rod. If we call $n_1 = \boldsymbol{n}\cdot\boldsymbol{d_1} = -n_x \sin\theta + n_y \cos\theta$ the internal shear force in the rod, we see that, using $n_3' = \kappa\, n_1$, (52) write $EI\,\theta''(s) = -n_1$ and can be integrated once to yield (53). Please also note that, using $\kappa = \theta'$, (53) leads to an integration by quadrature of the solution functions $\theta(s)$. Additionally, (53) also shows that the tension n_3 takes a maximum value along the rod at inflexion points $s = s_i$, where $\kappa(s_i) = 0$.

In the example cases presented here, the method is simply to write the invariant at different (carefully chosen) locations along the rod, and use the fact that the value of the invariant is the same everywhere, to exhibit relations between key quantities in the problem.

7.1. Vertical displacement

In the classical problem of the nonlinear dynamics of a point mass attached to a pendulum, the vertical angle $\theta(t)$ of the pendulum obeys the equation $\ell\ddot{\theta} = -g \sin\theta$, and writing the solution $\theta(t)$ requires the use of elliptic functions. However, to answer the question, illustrated in figure 2, of finding the maximum deflection angle θ_{max} as a function of the initial angular speed $\dot{\theta}_0$ does not necessitate the use of elliptic functions. The key point is to use the time conservation of the mechanical energy $E_{meca} = \frac{1}{2}\ell\dot{\theta}^2 - g\cos\theta$, write the value of E_{meca} at times $t = t_A$ and $t = t_B$ and find $\cos\theta_{max} = 1 - \ell\dot{\theta}_0^2/(2g)$. The Kirchhoff static-dynamic analogy (see (Kirchhoff, 1859), or (O'Reilly, 2017) for a modern treatment) tells us that we can carry out the same method to study the problem shown in figure 3, where a simply-supported Elastica is compressed with a force P and displays a deflection θ_0 at the supports. In this case, we have $n_x = -P$ and $n_y = 0$. Finding the values of the maximum vertical displacement y_M and maximum curvature κ_M would in principle require integrating (52) using elliptic functions, whereas writing the invariant (53) at point O and M directly yields

$$\kappa_M = \sqrt{\frac{2P}{EI}\,(1 - \cos\theta_0)}\,, \quad y_M = \sqrt{\frac{2EI}{P}\,(1 - \cos\theta_0)} \tag{54}$$

7.2. Frictionless contact

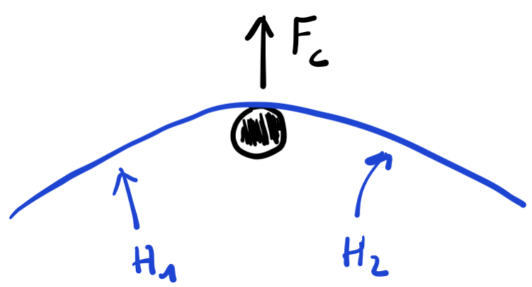

Figure 4: In the case of frictionless contact, the contact force applied from the obstacle onto the rod is perpendicular to the rod's tangent. The values H_1 and H_2, left and right of the contact point, are shown to be equal.

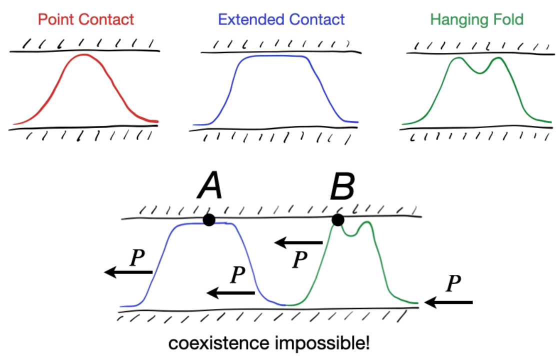

Figure 5: Among the possible configurations an Elastica buckling in a rectangular cavity may adopt, the use of the invariance of H enables us to rule out the coexistence of some of them.

We explained in section 6 that frictionless contact, continuous or not, leaves the values of the invariant unchanged. Therefore, in the case where the planar Elastica is in frictionless contact with an obstacle (or in self-contact), see figure 4, the invariant keeps the same value along the entire rod, that is $H_1 = H_2$ (see also jump conditions at obstacles in

(O'Reilly, 2017)). We use this property in the problem of an Elastica buckling inside a rectangular cavity, see figure 5. In this problem, it was shown that several configurations are encountered, namely the point-contact shape where the Elastica touches the wall at a localised value of the arclength, the extended-contact shape where contact happens for an interval of arclength values, and the hanging-fold shape where a blister is formed between two discrete contact points (Lubinski and Althouse, 1962; Chai, 1998; Domokos et al., 1997; Roman and Pocheau, 1999). In all these configurations H keeps a constant value, and if these configurations were to be found along the same rod, H would have to be the same everywhere.

We question the possibility of having both an extended-contact and a hanging-fold solutions coexisting along the same rod, see figure 5. The frictionless character of the wall interactions implies that the horizontal component of the internal force stays constant along the rod, $n_x = -P$, $\forall s$. In addition, the flat shape the extended-contact solution adopts as it is lying along the wall shows that the invariant at point A is equal to $H_A = -P$. Thus, writing the invariant at point B, where the deflection angle vanishes $\theta_B = 0$ but not the curvature $\kappa_B < 0$, yields $H_B = \frac{1}{2}\kappa_B^2 - P$ and demonstrates the impossibility of such a coexistence.

7.3. Sliding sleeves

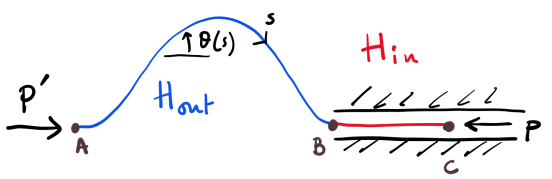

Figure 6: A planar Elastica is buckled through a frictionless sliding sleeve. The external forces P and P' at the right and left extremities do not match, due to the horizontal force coming from the sleeve at the exit point B.

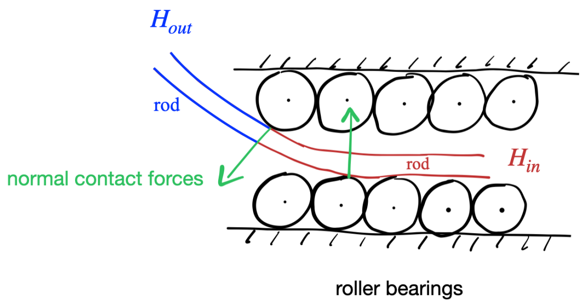

Figure 7: A closer look at the forces applied on the rod at the exit of the frictionless sliding sleeve, adapted from (Bigoni et al., 2015). The perpendicular (with respect to the rod's tangent) orientation of these forces implies the equality $H_{in} = H_{out}$, see sections 6 and 7.2.

In the last decade, it was shown that the buckling of an Elastica through a frictionless sliding sleeve exhibited a (somewhat counterintuitive) force jump at the exit of the sleeve, see for example (Bigoni et al., 2015; Dal Corso et al., 2017). We illustrate this in figure 6, where it is seen that the externally applied forces on the rod at points A and C do not match: $P \neq P'$. It is explained in (Bigoni et al., 2015; Cazzolli and Dal Corso, 2024) that the mismatch in horizontal forces is due to the contact force applied on the rod at the exit of the sleeve, see figure 7. The crucial point is that the forces from the roller bearings are frictionless and hence do not change the value of the invariant H, i.e. we have $H_{in} = H_{out}$, see figure 7. Thus, the relation between P and P' is easily obtained by writing H just before point B and at point C in figure 6

$$H_B = \frac{1}{2} EI\kappa_B^2 - P' \text{ and } H_C = 0 - P \tag{55a}$$

$$H_C = H_B \Rightarrow P' = P + \frac{1}{2}\kappa_B^2 \tag{55b}$$

7.4. The Elastica arm scale

The fact that the invariant H is conserved along the entire rod in rigid sleeve problems is handy for computing different properties of these systems at equilibrium. One such property is the horizontal tangent appearing when the Elastica arm scale (Bosi et al., 2014) is loaded at only one of its two extremities, see figure 8. Computing the value of H at point A yields $H_A = 0$, and computing the value of H at point C yields $H_C = \frac{1}{2}\kappa_C^2 - mg \sin\theta_C$. The absence of external torque loading at point C implies $\kappa_C = 0$ and thus the invariance $H_A = H_C$ proves that $\theta_C = 0$.

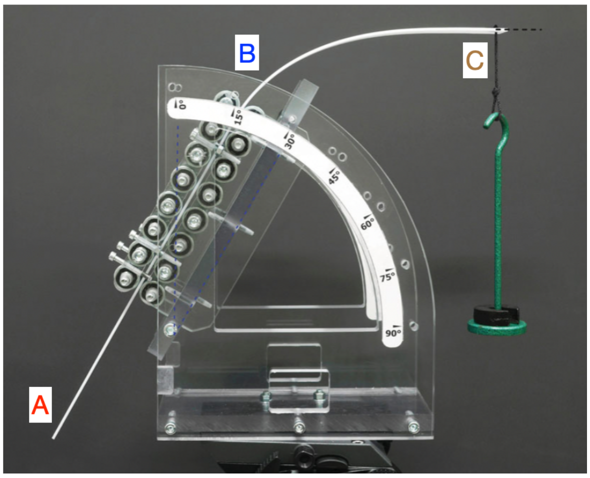

Figure 8: The Elastica arm scale, as introduced by Bosi et al. (2014). A weight of mass m is hung at the right extremity while the left extremity is unloaded. Use of the invariant easily shows that the rod's tangent is horizontal at point C. Image courtesy of Francesco Dal Corso.

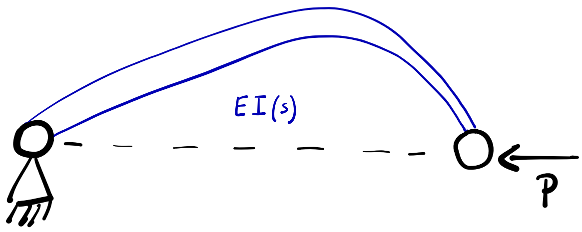

Figure 9: An Elastica with a cross-section of varying thickness. In this case the quantity $H(s)$ is not conserved along the rod.

7.5. A simple case where the invariant breaks down

In the so-called tapered case where the rod has a thickness which varies with arclength, see for example (Keller and Niordson, 1966), and hence a varying bending stiffness $EI(s)$, we show that the quantity $H(s)$ does depend on arclength. Consider for example the simply-supported Elastica of figure 9, for which the equilibrium equation (52) is replaced by

$$[EI(s)\,\theta'(s)]' = -P\sin\theta \tag{56}$$

In this case, we differentiate (53) and find

$$H'(s) = \frac{1}{2}EI'(s)\,\theta'^2(s) + EI(s)\,\theta'\,\theta'' + P\,\theta'\sin\theta = -\frac{1}{2}EI'(s)\,\theta'^2(s) \neq 0 \tag{57}$$

The fact that the quantity $H(s)$ loses its invariant property comes from the explicit dependence of the Lagrangian (51) with the arclength s, which kills the invariance of the Action (1) under the transformation (2b), a crucial hypothesis of Noether's theorem.

7.6. A 3D case with twist and continuous contact

We consider an inextensible, unshearable, naturally straight and untwisted rod with circular cross-section and isotropic elastic properties, $B_1 = B_2 = EI$ and $B_3 = GJ$. We study a 3D case where the rod is twisted and experiences self-contact, see figure 10. The rod is clamped at its left end and subject to an imposed rotation n and a pulling force T_{ext} at its right end. This setup is used for example in DNA single-molecule experiments (Bustamante et al., 2003; Strick et al., 1996) but also arises as an instability in textile yarns (Hearle, 2014). This complex configuration exhibits both point-wise and continuous contact (Coleman and Swigon, 2000; van der Heijden et al., 2003), but in the contact region the rod adopts an approximately double-helix shape. Due to self-contact, the helix radius is the radius R of the circular cross-section, and we note θ the helical angle, between the rod's tangent and the helical axis. The helix thus has a curvature $\kappa = \sqrt{\kappa_1^2 + \kappa_2^2} = (1/R)\,\sin^2\theta$, and using the helical shape approximation, it is possible to show (Thompson et al., 2002) that the contact pressure p, the twisting moment m_3, and the inner tension n_3 all essentially

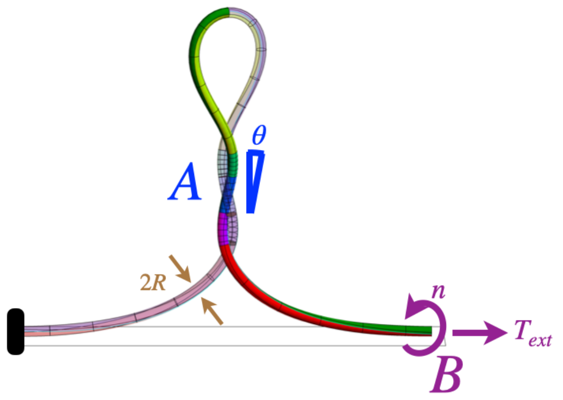

Figure 10: A rod is twisted and subject to an external tension T_{ext}. If the twist is large enough, the rod coils on itself, exhibiting plectonemes. A relation between the external tension and the coiling angle θ is found using the invariant H.

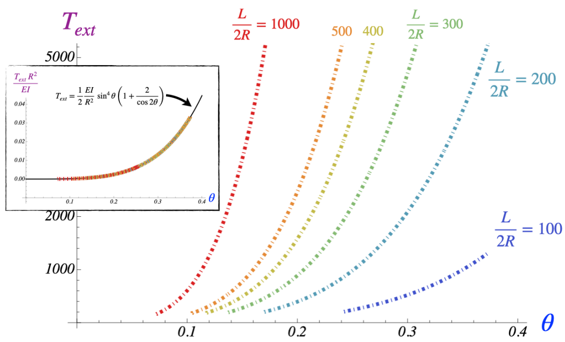

Figure 11: Several bifurcation branches are computed numerically for different slenderness ratios $L/(2R)$ and the relation between T_{ext} and θ is plotted and compared to (61), see inset.

depend on the helical angle θ

$$p_{helix} = \frac{EI}{R^3} \frac{\sin^4\theta}{\cos 2\theta} \tag{58a}$$

$$m_{3helix} = \frac{EI}{R} \frac{2\sin^3\theta \cos\theta}{\cos 2\theta} \tag{58b}$$

$$T_{helix} = \frac{EI}{R^2} \frac{\sin^4\theta}{\cos 2\theta} \tag{58c}$$

Thus, the helical angle θ appears as the crucial variable characterizing the mechanical state of the system, and we would like to compute θ as a function of the applied load T_{ext}. We derive such a relation using the invariant $H = \frac{1}{2}EI\kappa^2 + \frac{1}{2}\frac{m_3^2}{GJ} + n_3$, see (33) with $\hat{\boldsymbol{u}} = 0$, computed at points A and B. We first remark that we are in the case where $m_3'(s) = 0\ \forall s$ that is $m_{3A} = m_{3B} = m_{3helix}$, see (58b). At point B, no bending moment is applied, $\kappa_B = 0$, and the internal tension is equal to the external force, $n_{3B} = T_{ext}$. We therefore have

$$H_B = \frac{1}{2}\frac{m_{3helix}^2}{GJ} + T_{ext} \tag{59}$$

At point A, the curvature, twist, and tension are given by (58) and we have

$$H_A = \frac{1}{2}EI\frac{\sin^4\theta}{R^2} + \frac{1}{2}\frac{m_{3helix}^2}{GJ} + \frac{EI}{R^2}\frac{\sin^4\theta}{\cos 2\theta} \tag{60}$$

Equating $H_A = H_B$ yields

$$T_{ext} = \frac{1}{2}\frac{EI}{R^2}\sin^4\theta\left(1 + \frac{2}{\cos 2\theta}\right) \tag{61}$$

We performed numerical shooting simulations for different rod's slenderness ratios $L/(2R) = 100\ldots1000$, in which the end-to-end distance is fixed and the number of turns is varied from $n = 4$ up to $n \simeq 10, 20$, or 50. We record the force T_{ext} and the average value of the helical angle θ, and verify both the $1/R^2$ scaling of the force and the approximation provided by (61), see figure 11.

7.7. The invariant in the presence of an external force field

In this section, we study the case in which an external conservative force field is applied to the rod. Manning and Bulman (2005) introduced a soft-wall repulsion to deal with the wall-constrained buckling scenario presented in

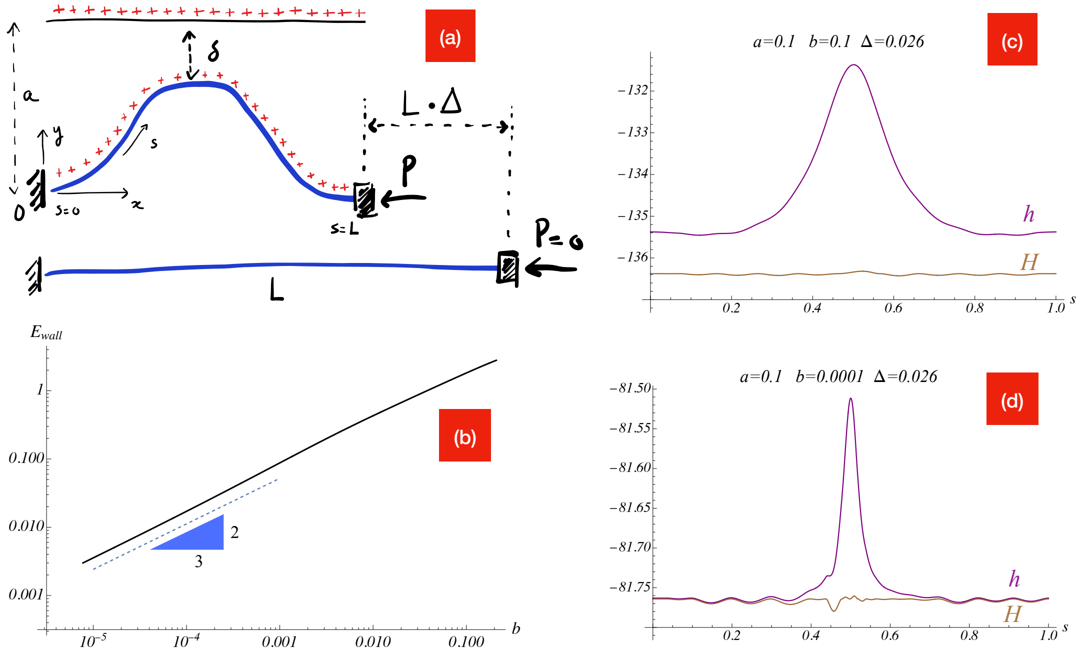

Figure 12: (a) The buckling of a planar Elastica constrained by a horizontal upper wall is studied using the long-range interaction potential (64). (b) Total interaction energy (69) as the 'range' b of the potential is decreased, with the limit $b \to 0$ corresponding to the hard-wall limit. (c) and (d) Plot of the arclength invariant H (67) together with the non-invariant function $h(s)$ for two different b values. We see that as b is decreased, the difference between H and $h(s)$ becomes smaller and that the constant H value tends toward the hard-wall limit -73.7. Fixed parameters $L = 1$, $EI = 1$, $a = 0.1$, and $\Delta = 0.026$.

figure 12-a. This corresponds to the buckling of a planar Elastica, subject to an imposed displacement Δ, constrained by an upper horizontal wall lying at a vertical distance a from the clamps. In the references cited in section 7.2, the authors used a frictionless hard-wall contact approach where

$$y(s) \leq a \quad \forall s \tag{62}$$

As explained earlier, this contact condition is treated by introducing the KKT term $-F_c[a - y(s)]$ in the Lagrangian (51), the Lagrange multiplier F_c corresponding to the contact force. In the case that the Elastica shape comprises a single arch and the contact with the upper wall is pointwise, the vertical component $n_y(s)$ of the internal force experiences a jump at $s = s_c$

$$n_y(s_c^+) - n_y(s_c^-) = F_c \tag{63}$$

with symmetry imposing $s_c = 1/2$.

Manning and Bulman (2005) replaced the contact condition (62) by a soft-wall (a.k.a. barrier) potential

$$W_{ext}(y) = \frac{b}{a - y(s)} \tag{64}$$

which is added to the total potential energy V of the rod, see (14), and therefore to the Lagrangian (51). In this model, the vertical component $n_y(s)$ no longer jumps at $s = 1/2$ but varies along the length of the rod

$$\left(\frac{\partial \mathcal{L}}{\partial y'}\right)' = \frac{\partial \mathcal{L}}{\partial y} \Rightarrow n_y'(s) = \frac{\partial W_{ext}}{\partial y} = \frac{b}{(a - y(s))^2} \tag{65}$$

Intuitively, this soft-wall approach can be interpreted as if the wall and the Elastica would be electrostatically charged with like charges and would therefore repel each other from a distance. The central point of the soft-wall approach is that, as b is made smaller, the computed equilibrium shape converges toward the shape obtained with the hard-wall contact condition (62) and

$$n_y(L) - n_y(0) = b \int_0^L \frac{ds}{(a-y(s))^2} \underset{b\to 0}{\longrightarrow} F_c \tag{66}$$

Morevoer, the gap $\delta = a - y(1/2)$, see figure 12, also decreases to zero as $b \to 0$. Note that the horizontal component $n_x(s)$ of the internal force is invariant $n_x'(s) = 0\ \forall s$ and set by the external compression force P, $n_x = -P$.

In this soft-wall approach, the arclength invariant reads

$$H = h(s) - W_{ext}(y) \quad \text{with} \quad h(s) = \frac{1}{2}\theta'^2(s) - P\cos\theta - n_y(s)\sin\theta \tag{67}$$

with $H'(s) = 0\ \forall s$ but $h'(s) \neq 0$. We fix the parameter values

$$L = 1\,, \quad EI = 1\,, \quad a = 0.1\,, \quad \Delta = 0.026 \tag{68}$$

and numerically compute the equilibrium using the soft-wall approach with $b = 0.1$ and $b = 10^{-4}$ to see that the term $-W_{ext}(y)$ in (67) is necessary to achieve uniformity of H, see figure 12-c and d. Now in the case of hard-wall contact, we have explained in section 6 that no extra term is required, and the formula for the invariant is indeed that of h in (67). This can be understood by showing that the importance of W_{ext} decreases as $b \to 0$, as can be seen when comparing figures 12-c and d. To make this more quantitative, we numerically compute

$$E_{wall} = b \int_0^1 \frac{ds}{a - y(s)} \tag{69}$$

and plot it as b is varied in figure 12-b. We see that $E_{wall}(b) \sim b^{2/3}$ for small b values. This scaling can be understood in the following way. We consider the soft-wall solution as b is decreased toward zero. In this limit, the denominators in the integrands of (66) and (69) are taking small values when s is near $s_c = 1/2$, and therefore these integrals are dominated by the behaviour of the function $y(s)$ near $s = s_c$. A Taylor expansion yields

$$y(s) = a - \delta + \frac{1}{2}\kappa_c\,(s - 1/2)^2 + \ldots \tag{70}$$

As $b \to 0$, δ and κ_c converge toward the hard-wall limit, $\delta \to 0$ and $\kappa_c \to -1.54$ for parameters values in (68). Plugging this expansion for $y(s)$ into the integrals (66) and (69) we find

$$\int_0^L \frac{ds}{(a-y(s))^2} = \frac{\pi}{\sqrt{8\kappa_c}}\,\delta^{-3/2} + O(\delta^{-1}) \tag{71a}$$

$$\int_0^L \frac{ds}{a-y(s)} = \frac{\pi}{\sqrt{2\kappa_c}}\,\delta^{-1/2} + O(\delta^{0}) \tag{71b}$$

Considering the leading order of (66) when $b \to 0$, for which $F_c = 18.1$ for parameters values in (68), we see (71a) implies $b \sim \delta^{3/2}$ and consquently (71b) implies $E_{wall}(b) \sim b^{2/3}$.

Finally, we remark that for every b value, the curve $H(s)$ should be strictly flat. The size of the undulations seen in figures 12-c and d is then a measure of the quality of the numerical solution.

8. Dynamics

The angular velocity is noted $\boldsymbol{\omega}(s,t) = \omega_1 \boldsymbol{d_1} + \omega_2 \boldsymbol{d_2} + \omega_3 \boldsymbol{d_3}$ and we have

$$\dot{\boldsymbol{d}}_{\boldsymbol{1}}(s,t) = \boldsymbol{\omega} \times \boldsymbol{d_1} \tag{72a}$$

$$\dot{\boldsymbol{d}}_{\boldsymbol{2}}(s,t) = \boldsymbol{\omega} \times \boldsymbol{d_2} \tag{72b}$$

$$\dot{\boldsymbol{d}}_{\boldsymbol{3}}(s,t) = \boldsymbol{\omega} \times \boldsymbol{d_3} \tag{72c}$$

The three vectorial relations (72) are constraints for the three scalar components ω_1, ω_2, ω_3 and can thereof be rewritten as

$$\omega_1 = \dot{\boldsymbol{d}}_{\boldsymbol{2}} \cdot \boldsymbol{d}_{\boldsymbol{3}}\,, \quad \omega_2 = \dot{\boldsymbol{d}}_{\boldsymbol{3}} \cdot \boldsymbol{d}_{\boldsymbol{1}}\,, \quad \omega_3 = \dot{\boldsymbol{d}}_{\boldsymbol{1}} \cdot \boldsymbol{d}_{\boldsymbol{2}} \tag{73}$$

To derive dynamical equations for the elastic rod, we complement the Lagrangian (19) with the linear and angular kinetic energies

$$\mathcal{L}_d = \mathcal{L} - K - \lambda_{\omega_1}(\dot{\boldsymbol{d}}_{\boldsymbol{2}} \cdot \boldsymbol{d}_{\boldsymbol{3}} - \omega_1) - \lambda_{\omega_2}(\dot{\boldsymbol{d}}_{\boldsymbol{3}} \cdot \boldsymbol{d}_{\boldsymbol{1}} - \omega_2) - \lambda_{\omega_3}(\dot{\boldsymbol{d}}_{\boldsymbol{1}} \cdot \boldsymbol{d}_{\boldsymbol{2}} - \omega_3) \tag{74a}$$

$$\text{with } K = \frac{1}{2}\rho S\,\dot{\boldsymbol{r}}^2 + \frac{1}{2}I_1\omega_1^2 + \frac{1}{2}I_2\omega_2^2 + \frac{1}{2}I_3\omega_3^2 \tag{74b}$$

where I_1 and I_2 are the moment of inertia of the cross-section about $\boldsymbol{d}_{\boldsymbol{1}}$ and $\boldsymbol{d}_{\boldsymbol{2}}$, and $I_3 = I_1 + I_2$ is the polar moment of intertia, about $\boldsymbol{d}_{\boldsymbol{3}}$. And the action is

$$\mathcal{A}(\boldsymbol{r}, \boldsymbol{d}_{\boldsymbol{1}}, \boldsymbol{d}_{\boldsymbol{2}}, \boldsymbol{d}_{\boldsymbol{3}}, u_1, u_2, u_3, v_1, v_2, v_3, \omega_1, \omega_2, \omega_3) = \int_{t_1}^{t_2}\int_0^L \mathcal{L}_d\, ds\, dt \tag{75}$$

8.1. Euler-Lagrange equations

We use the principle of least action to obtain the equations for the dynamics of the elastic rod. Necessary conditions for the vanishing of the first variation of (75) are the following Euler-Lagrange equations. Equations (21b), (21c), (21d), (21e), (21f), and (21g) stay unchanged and here also we identify the Lagrange multiplier $\boldsymbol{\lambda}_{\boldsymbol{r}}$ with the internal force vector $\boldsymbol{n} = \boldsymbol{\lambda}_{\boldsymbol{r}}$. Furthermore, the derivation with regard to the ω_i unravel a new constitutive relation

$$\frac{\partial \mathcal{L}_d}{\partial \omega_1} = 0 \Rightarrow \lambda_{\omega_1} = I_1\,\omega_1 \tag{76}$$

$$\frac{\partial \mathcal{L}_d}{\partial \omega_2} = 0 \Rightarrow \lambda_{\omega_2} = I_2\,\omega_2 \tag{77}$$

$$\frac{\partial \mathcal{L}_d}{\partial \omega_3} = 0 \Rightarrow \lambda_{\omega_3} = I_3\,\omega_3 \tag{78}$$

where we interpret the Lagrange multipliers λ_{ω_i} as the components of the angular momentum $\boldsymbol{\pi} = \lambda_{\omega_1}\boldsymbol{d}_{\boldsymbol{1}} + \lambda_{\omega_2}\boldsymbol{d}_{\boldsymbol{2}} + \lambda_{\omega_3}\boldsymbol{d}_{\boldsymbol{3}}$, which we will now write π_i. The linear momentum equation, (21a), is now

$$\frac{\partial \mathcal{L}_d}{\partial \boldsymbol{r}} = \left(\frac{\partial \mathcal{L}_d}{\partial \boldsymbol{r}'}\right)' + \overset{\bullet}{\left(\frac{\partial \mathcal{L}_d}{\partial \dot{\boldsymbol{r}}}\right)} \Rightarrow \boldsymbol{n}'(s) + \boldsymbol{f}_{\text{ext}} = \rho S\,\ddot{\boldsymbol{r}} \tag{79}$$

Euler-Lagrange equations for the director basis $(\boldsymbol{d}_{\boldsymbol{1}}, \boldsymbol{d}_{\boldsymbol{2}}, \boldsymbol{d}_{\boldsymbol{3}})$ are changed to

$$\frac{\partial \mathcal{L}_d}{\partial \boldsymbol{d}_{\boldsymbol{1}}} = \left(\frac{\partial \mathcal{L}_d}{\partial \boldsymbol{d}'_{\boldsymbol{1}}}\right)' + \overset{\bullet}{\left(\frac{\partial \mathcal{L}_d}{\partial \dot{\boldsymbol{d}}_{\boldsymbol{1}}}\right)} \Rightarrow \lambda_{u_3}\,\boldsymbol{d}'_{\boldsymbol{2}} - \lambda_{u_2}\,\boldsymbol{d}'_{\boldsymbol{3}} + \lambda'_{u_3}\boldsymbol{d}_{\boldsymbol{2}} + \boldsymbol{\lambda}_{\boldsymbol{r}}v_1 + \lambda_{11}\boldsymbol{d}_{\boldsymbol{1}} - \lambda_{12}\boldsymbol{d}_{\boldsymbol{2}} - \lambda_{31}\boldsymbol{d}_{\boldsymbol{3}} + \pi_2\dot{\boldsymbol{d}}_{\boldsymbol{3}} - \pi_3\dot{\boldsymbol{d}}_{\boldsymbol{2}} - \dot{\pi}_3\boldsymbol{d}_{\boldsymbol{2}} = 0 \tag{80a}$$

$$\frac{\partial \mathcal{L}_d}{\partial \boldsymbol{d}_{\boldsymbol{2}}} = \left(\frac{\partial \mathcal{L}_d}{\partial \boldsymbol{d}'_{\boldsymbol{2}}}\right)' + \overset{\bullet}{\left(\frac{\partial \mathcal{L}_d}{\partial \dot{\boldsymbol{d}}_{\boldsymbol{2}}}\right)} \Rightarrow \lambda_{u_1}\,\boldsymbol{d}'_{\boldsymbol{3}} - \lambda_{u_3}\,\boldsymbol{d}'_{\boldsymbol{1}} + \lambda'_{u_1}\boldsymbol{d}_{\boldsymbol{3}} + \boldsymbol{\lambda}_{\boldsymbol{r}}v_2 + \lambda_{22}\boldsymbol{d}_{\boldsymbol{2}} - \lambda_{23}\boldsymbol{d}_{\boldsymbol{3}} - \lambda_{12}\boldsymbol{d}_{\boldsymbol{1}} + \pi_3\dot{\boldsymbol{d}}_{\boldsymbol{1}} - \pi_1\dot{\boldsymbol{d}}_{\boldsymbol{3}} - \dot{\pi}_1\boldsymbol{d}_{\boldsymbol{3}} = 0 \tag{80b}$$

$$\frac{\partial \mathcal{L}_d}{\partial \boldsymbol{d}_{\boldsymbol{3}}} = \left(\frac{\partial \mathcal{L}_d}{\partial \boldsymbol{d}'_{\boldsymbol{3}}}\right)' + \overset{\bullet}{\left(\frac{\partial \mathcal{L}_d}{\partial \dot{\boldsymbol{d}}_{\boldsymbol{3}}}\right)} \Rightarrow \lambda_{u_2}\,\boldsymbol{d}'_{\boldsymbol{1}} - \lambda_{u_1}\,\boldsymbol{d}'_{\boldsymbol{2}} + \lambda'_{u_2}\boldsymbol{d}_{\boldsymbol{1}} + \boldsymbol{\lambda}_{\boldsymbol{r}}v_3 + \lambda_{33}\boldsymbol{d}_{\boldsymbol{3}} - \lambda_{31}\boldsymbol{d}_{\boldsymbol{1}} - \lambda_{23}\boldsymbol{d}_{\boldsymbol{2}} + \pi_1\dot{\boldsymbol{d}}_{\boldsymbol{2}} - \pi_2\dot{\boldsymbol{d}}_{\boldsymbol{1}} - \dot{\pi}_2\boldsymbol{d}_{\boldsymbol{1}} = 0. \tag{80c}$$

Analogous manipulations as in the static case lead to

$$m'_1(s) - u_3m_2 + u_2m_3 - v_3n_2 + v_2n_3 = \dot{\pi}_1 + \omega_2\pi_3 - \omega_3\pi_2 \tag{81a}$$

$$m'_2(s) - u_1m_3 + u_3m_1 - v_1n_3 + v_3n_1 = \dot{\pi}_2 + \omega_3\pi_1 - \omega_1\pi_3 \tag{81b}$$

$$m'_3(s) - u_2m_1 + u_1m_2 - v_2n_1 + v_1n_2 = \dot{\pi}_3 + \omega_1\pi_2 - \omega_2\pi_1 \tag{81c}$$

and, using (11), yields the vectorial relation

$$\boldsymbol{m}'(s,t) + \boldsymbol{r}'(s,t) \times \boldsymbol{n}(s,t) = \dot{\boldsymbol{\pi}}(s,t) \tag{82}$$

8.2. Invariants in the dynamics case

The same symmetries as in the static case hold, except for the one of Section 5.4, basically because the force vector $\boldsymbol{n}$ is no longer constant.

8.2.1. Configuration translation

Just as in Section 5.2, in the absence of any external force field, $W_{\text{ext}} = 0$, the transformation $\tilde{\boldsymbol{r}} = \boldsymbol{r} + \boldsymbol{a}$ leaves the Lagrangian (74a) invariant. Consequently, (4a) yields

$$\left[\boldsymbol{a} \cdot \frac{\partial \mathcal{L}_d}{\partial \dot{\boldsymbol{r}}}\right]^\bullet + \left[\boldsymbol{a} \cdot \frac{\partial \mathcal{L}_d}{\partial \boldsymbol{r}'}\right]' = 0 \quad \forall \boldsymbol{a} \quad \Rightarrow \quad \boldsymbol{n}' = \rho S \ddot{\boldsymbol{r}} \tag{83}$$

which is just the dynamics equation (79) when $W_{\text{ext}} = 0$. See also Eq. (2.12) in (Maddocks and Dichmann, 1994).

8.2.2. Configuration rotation

Still in the absence of any external force field, the rotation transformation (38) leaves the Lagrangian (74a) invariant. Consequently, (4a) yields

$$\left[\boldsymbol{b} \times \boldsymbol{r} \cdot \frac{\partial \mathcal{L}_d}{\partial \dot{\boldsymbol{r}}} + \boldsymbol{b} \times \boldsymbol{d}_{1,2,3} \cdot \frac{\partial \mathcal{L}_d}{\partial \dot{\boldsymbol{d}}_{1,2,3}}\right]^\bullet + \left[\boldsymbol{b} \times \boldsymbol{r} \cdot \frac{\partial \mathcal{L}_d}{\partial \boldsymbol{r}'} + \boldsymbol{b} \times \boldsymbol{d}_{1,2,3} \cdot \frac{\partial \mathcal{L}_d}{\partial \boldsymbol{d}'_{1,2,3}}\right]' = 0 \tag{84a}$$

$$[-\boldsymbol{b} \cdot \boldsymbol{r} \times \rho S \dot{\boldsymbol{r}} - \boldsymbol{b} \cdot \boldsymbol{\pi}]^\bullet + [\boldsymbol{b} \cdot \boldsymbol{r} \times \boldsymbol{n} + \boldsymbol{b} \cdot \boldsymbol{m}]' = 0 \quad \forall \boldsymbol{b} \tag{84b}$$

$$-[\boldsymbol{r} \times \rho S \dot{\boldsymbol{r}} + \boldsymbol{\pi}]^\bullet + [\boldsymbol{r} \times \boldsymbol{n} + \boldsymbol{m}]' = 0 \tag{84c}$$

which may be obtained by combining (79) and (82) with $W_{\text{ext}} = 0$. See also Eq. (2.14) in (Maddocks and Dichmann, 1994).

8.2.3. Configuration rotation around the section normal

In the presence or absence of an external force field, we now consider the transformation (45) in the case where $A_1 = A_2$, $B_1 = B_2$, $\hat{u}_1 = 0$, $\hat{u}_2 = 0$, $\hat{v}_1 = 0$, and $\hat{v}_2 = 0$. This transformation leaves the Lagrangian (74a) unchanged, and consequently, from (4a), we have

$$\left[\boldsymbol{d}_3 \times \boldsymbol{d}_1 \cdot \frac{\partial \mathcal{L}_d}{\partial \dot{\boldsymbol{d}}_1} + \boldsymbol{d}_3 \times \boldsymbol{d}_2 \cdot \frac{\partial \mathcal{L}_d}{\partial \dot{\boldsymbol{d}}_2} + u_2 \frac{\partial \mathcal{L}_d}{\partial \dot{u}_1} - u_1 \frac{\partial \mathcal{L}_d}{\partial \dot{u}_2} + v_2 \frac{\partial \mathcal{L}_d}{\partial \dot{v}_1} - v_1 \frac{\partial \mathcal{L}_d}{\partial \dot{v}_2}\right]^\bullet + \left[\boldsymbol{d}_3 \times \boldsymbol{d}_1 \cdot \frac{\partial \mathcal{L}_d}{\partial \boldsymbol{d}'_1} + \boldsymbol{d}_3 \times \boldsymbol{d}_2 \cdot \frac{\partial \mathcal{L}_d}{\partial \boldsymbol{d}'_2} + u_2 \frac{\partial \mathcal{L}_d}{\partial u'_1} - u_1 \frac{\partial \mathcal{L}_d}{\partial u'_2} + v_2 \frac{\partial \mathcal{L}_d}{\partial v'_1} - v_1 \frac{\partial \mathcal{L}_d}{\partial v'_2}\right]' = 0 \tag{85a}$$

$$-[\pi_3(s,t)]^\bullet + [m_3(s,t)]' = 0 \tag{85b}$$

Please note that this results hold in the case where $\hat{u}_3 \neq 0$ and $\hat{v}_3 \neq 0$ as long as they are constant and uniform. See also Eq. (4.5) in (Maddocks and Dichmann, 1994).

8.2.4. Arclength translation

As the Lagrangian (74a) does not explicitly depend on s, the conservation law (4b) holds along a dynamic trajectory. Recalling $\boldsymbol{q} = (\boldsymbol{r}, \boldsymbol{d}_1, \boldsymbol{d}_2, \boldsymbol{d}_3, u_1, u_2, u_3, v_1, v_2, v_3)$, we obtain the 'density-flux' conservation identity

$$-[\boldsymbol{\pi} \cdot \boldsymbol{u} + \rho S \dot{\boldsymbol{r}} \cdot \boldsymbol{r}']^\bullet + [H + K]' = 0 \tag{86}$$

with H given by (29) and K given by (74b). See also Eq. (3.2) in (Maddocks and Dichmann, 1994). The relation (86) may be used as a validation test for numerical codes.

8.2.5. Time translation

As the Lagrangian (74a) does not explicitly depend on t, the conservation law (4c) holds along a dynamic trajectory. Recalling $\boldsymbol{q} = (\boldsymbol{r}, \boldsymbol{d_1}, \boldsymbol{d_2}, \boldsymbol{d_3}, u_1, u_2, u_3, v_1, v_2, v_3)$, we obtain

$$-[K+V]^{\bullet} + [\boldsymbol{m}\cdot\boldsymbol{\omega} + \boldsymbol{n}\cdot\dot{\boldsymbol{r}}]' = 0 \tag{87}$$

with V given by (14) and K given by (74b). See also Eq. (2.19) in (Maddocks and Dichmann, 1994). The relation (87), once integrated over the entire rod, shows that the total mechanical energy

$$\int_0^L (K+V)\, ds \tag{88}$$

is time-invariant in the case of conservative boundary conditions ($\dot{\boldsymbol{r}}(0, L) = 0 = \boldsymbol{\omega}(0, L)$), such a clamps or if the rod is circularly closed on itself, or free ends $\boldsymbol{m}(0, L) = 0 = \boldsymbol{n}(0, L)$.

9. Vibrations

Here, we show that vibration equations for elastic rods may be obtained through a variational approach and, as a result, we display the associated invariant. We illustrate this in the case of the vibrations of the planar Elastica but it can be straightforwardly generalised to the 3D case. For the sake of simplicity, we restrict to the naturally straight ($\hat{\kappa} = 0$), inextensible ($v_3(s) = 1\ \forall s, t$), unshearable ($v_1(s) = v_2(s) = 0\ \forall s, t$) case. We start with the 2D version of (74a)

$$\mathcal{L}_d^{2D} = \frac{1}{2}\, EI\, \kappa(s,t)^2 - \frac{1}{2}\rho S\,(\dot{x}^2 + \dot{y}^2) + \lambda_1(s,t)\,(x' - \cos\theta) + \lambda_2(s,t)\,(y' - \sin\theta) + \lambda_3(s,t)\,(\theta' - \kappa) \tag{89}$$

where the first term is the internal bending energy, the second is the translational kinetic energy (for simplicity, we do not consider here rotational inertia, $I_{1,2,3} = 0$), and the last three terms correspond to the kinematics constraints

$$x' = \cos\theta\,,\ y' = \sin\theta\,,\ \theta' = \kappa \tag{90}$$

Anticipating the interpretation of the Lagrange multiplier $\lambda_{1,2,3}$, we introduce the horizontal and vertical components of the internal force vector $\lambda_1 = n_x(s,t)$, $\lambda_2 = n_y(s,t)$, and the internal moment $\lambda_3 = m(s,t)$. The equations for the dynamics of the planar Elastica are then obtained by applying the least action principle to

$$\mathcal{A}^{2D}[\boldsymbol{q}(s,t)] = \int_{t_1}^{t_2}\int_0^L \mathcal{L}_d^{2D}\, ds\, dt \tag{91}$$

with $\boldsymbol{q}(s,t) = (x(s,t), y(s,t), \theta(s,t), \kappa(s,t))$, see section Appendix B.

To study the small-amplitude vibrations around a pre-computed equilibrium $\boldsymbol{q}_e$, we introduce the ansatz

$$\boldsymbol{q}(s,t) = \boldsymbol{q}_e(s) + \epsilon\bar{\boldsymbol{q}}(s)\cos\omega t\,,\ n_{x,y}(s,t) = n_{xe,ye}(s) + \epsilon\,\bar{n}_{x,y}(s)\cos\omega t\,,\ m(s,t) = m_e(s) + \epsilon\,\bar{m}(s)\cos\omega t \tag{92}$$

into (91) and keep terms up to order ϵ^2. We obtain

$$\mathcal{A}^{2D}[\bar{\boldsymbol{q}}(s)] = \mathcal{A}_e^{2D} + \epsilon\mathcal{A}_1^{2D}[\bar{\boldsymbol{q}}(s)] + \epsilon^2\mathcal{A}_2^{2D}[\bar{\boldsymbol{q}}(s)] + \ldots \tag{93}$$

The Action $\mathcal{A}_e^{2D}$ is here a 'constant', given quantity, and is therefore not subject to optimisation. The Action $\mathcal{A}_1^{2D}$ contains a $\cos\omega t$ term which makes it vanish when the time integration is either taken over a period, $t_2 = t_1 + 2\pi/\omega$, or over a long time interval. We are then left with the Action $\mathcal{A}_2^{2D}$ which reads

$$\mathcal{A}_2^{2D} = \int_{t_1}^{t_2}\cos^2\omega t \int_0^L \mathcal{L}_{vib}^{2D}\, ds\, dt \tag{94a}$$

$$\mathcal{L}_{vib}^{2D}[\bar{\boldsymbol{q}}(s)] = \frac{1}{2}EI\,\bar{\kappa}^2 - \frac{1}{2}\rho S\,\omega^2(\bar{x}^2 + \bar{y}^2) + \frac{1}{2}\bar{\theta}^2(n_{xe}\cos\theta_e + n_{ye}\sin\theta_e) + \bar{n}_x(\bar{x}' + \bar{\theta}\sin\theta_e) + \bar{n}_y(\bar{y}' - \bar{\theta}\cos\theta_e) + \bar{m}(\bar{\theta}' - \bar{\kappa}) \tag{94b}$$

and Euler-Lagrange equations applied to $\mathcal{L}^{2D}_{vib}$ yield the classical vibration equations (B.4). We emphasize that the equilibrium solution $\theta_e(s)$ is a given function when working with the Lagrangian $\mathcal{L}^{2D}_{vib}$ and that a Noether arclength invariant will only exist in the case that the equilibrium shape of the beam is straight, $\theta_e'(s) = 0\ \forall s$. In such a case the invariant reads

$$H^{2D}_{vib} = \frac{\partial \mathcal{L}^{2D}_{vib}}{\partial \bar{\boldsymbol{q}}'} \cdot \bar{\boldsymbol{q}}' - \mathcal{L}^{2D}_{vib} \tag{95a}$$

$$= \frac{1}{2}\, EI\,\bar{\theta}'^2 - \bar{\theta}\left(\bar{n}_x\ \sin\theta_e - \bar{n}_y\ \cos\theta_e\right) + \frac{1}{2}\rho S\,\omega^2\left(\bar{x}^2 + \bar{y}^2\right) - \frac{1}{2}\bar{\theta}^2\left(n_{xe}\cos\theta_e + n_{ye}\sin\theta_e\right) \tag{95b}$$

In the case of a horizontal equilibrium ($\theta_e(s) = 0\ \forall s$) of an Elastica under a compressive force $n_{xe} = -P$, $n_{ye} = 0$, the vibration equations simplify to the classical form

$$EI\,\bar{y}'''' + P\,\bar{y}'' - \rho S\,\omega^2\,\bar{y} = 0 \tag{96}$$

and the invariant reads

$$H^{2D}_{vib} = \frac{1}{2}EI\,\bar{y}''^2 + \frac{1}{2}\rho S\,\omega^2\,\bar{y}^2 - \frac{1}{2}P\,\bar{y}^2 - EI\,\bar{y}'\,\bar{y}''' \tag{97}$$

a quantity that we have not managed to find in the existing literature.

10. Discussion and Conclusion

We have provided a comprehensive variational approach for elastic rods and ribbons where the continuous kinematic constraints play an important role, as this is only when they are explicitly included in the Lagrangian of the problem that Euler-Lagrange equations are straightforwardly derived. Moreover we showed that such a Lagrangian can be used to unravel conserved quantities or relations in the statics or dynamics of elastic rods and ribbons. Additionally, we have put forward an alternative Lagrangian approach where rotation constraints are automatically fulfilled, leading to more compact Euler-Lagrange equations and straightforward Noether invariants. Using Noether's 1918 theorem, we have recovered all known static and dynamic invariants and generalised the conditions under which they exist. More precisely, the arclength invariant, usually referred to as the Hamiltonian invariant, stands up to the adjunction of conservative external loading (e.g. gravity, electrostatics) and frictionless contact, but also holds in the case of Wunderlich, Sadowsky, and Ribext ribbon models. Furthermore, we illustrated the use of the arclength invariant in different 2D and 3D setups where it proves remarkably efficient in providing key quantities or relations in difficult problems. In one such problem, the sliding sleeve, the invariant provides an easy explanation of the somewhat mysterious force applied to the rod at the entry/exit of the sleeve. Finally, we have introduced a variational approach to vibrations of elastic rods and computed a first integral to the vibration mode equation of a straight cantilever.

Future work could include, among others, (*i*) the search for a more general invariant in the case of vibrations (that is, not restricted to the case of vibrations around a straight equilibrium), (*ii*) the case of contact in the presence of friction, where the invariant is sometimes increasing exponentially with s instead of being constant, (*iii*) the search of other space and/or time transformations that keep the Action unchanged (see for example Eq. (12) in (Kienzler and Herrmann, 1986)) thereby providing new invariants, (*iv*) the search for a clever use of the two dynamics invariants (86),(87) either for validation of codes for the dynamics of rods or to study their dynamical behavior.

Acknowledgments

We thank Aziz Hamdouni for discussions on Lie Groups and invariants, Olivier Thomas for discussions on vibrations of elastic rods, and Thibaut Métivet and Émile Hohnadel for discussions and references on reduced $\mathcal{SO}(3)$ parametrisations of rigid bodies.

Appendix A. $\mathcal{SO}(3)$ computations

Appendix A.1. Reminder: Euler-Lagrange and Noether's theorem on $\mathbb{R}^n$

Let $\boldsymbol{q} \in \mathbb{R}^n$ the n independent generalised coordinates of a mechanical system, and $\boldsymbol{q}' = \frac{\partial \boldsymbol{q}}{\partial s} \in \mathbb{R}^n$ the corresponding generalised velocities. With $\mathcal{L}(\boldsymbol{q}, \boldsymbol{q}')$ the Lagrangian functional depending on these generalised coordinates and velocities, the (classical) Euler-Lagrange equation read

$$\frac{\mathrm{d}}{\mathrm{d}s}\frac{\partial \mathcal{L}}{\partial \boldsymbol{q}'} - \frac{\partial \mathcal{L}}{\partial \boldsymbol{q}} = 0. \tag{A.1}$$

The Euler-Lagrange equation (A.1) results from the stationarity of the action

$$\mathcal{A}(\boldsymbol{q}, \boldsymbol{q}') = \int_0^L \mathcal{L}(\boldsymbol{q}, \boldsymbol{q}')\mathrm{d}s, \tag{A.2}$$

upon trajectories $\boldsymbol{q}, \boldsymbol{q}'$. It can be proved using integration by parts, which especially yields the following conditions on the boundary terms,

$$\left[\frac{\partial \mathcal{L}}{\partial \boldsymbol{q}'} \cdot \delta \boldsymbol{q}\right]_0^L = 0, \tag{A.3}$$

i.e.

$$\frac{\partial \mathcal{L}}{\partial \boldsymbol{q}'}(0) = 0 \qquad \text{or } \delta \boldsymbol{q}(0) = 0 \tag{A.4}$$

$$\frac{\partial \mathcal{L}}{\partial \boldsymbol{q}'}(L) = 0 \qquad \text{or } \delta \boldsymbol{q}(L) = 0, \tag{A.5}$$

which, for a mechanical system, can be interpreted as the vanishing of either the infinitesimal displacement $\delta \boldsymbol{q}$ or the applied force $\frac{\partial \mathcal{L}}{\partial \boldsymbol{q}'}$ at a boundary point.

Appendix A.2. Euler-Lagrange on $\mathbb{R}^n \times \mathcal{SO}(3)$

It is noteworthy that equations (A.1) are only valid for generalised coordinates satisfying $\frac{\partial}{\partial s}\boldsymbol{q} = \boldsymbol{q}'$, and the compatibility equation $\frac{\partial}{\partial s}\delta \boldsymbol{q} = \delta \boldsymbol{q}'$. This formula is thus applicable to translational degrees of freedom (such as positions), but not for rotational degrees of freedom, such as rotation matrices $R \in \mathcal{SO}(3)$, unless adding constraints to the Lagrangian formulation to maintain R in $\mathcal{SO}(3)$, see Section 4 of this paper. Without any constraint, if one chooses $\boldsymbol{q} = R$, then the compatibility condition is not valid: one cannot swap derivation and perturbation on $\mathcal{SO}(3)$. To do so, a supplementary compatibility condition has to be satisfied.

In contrast, if one uses the Euler-Poincaré parametrisation of rotations, i.e. $\mathring{\mathcal{L}}(R, \bar{\boldsymbol{u}})$ with $R' = R[\bar{\boldsymbol{u}}]_\times$, new Euler-Lagrange equations can be derived from the least action principle, by imposing the compatibility condition

$$\delta \bar{\boldsymbol{u}} = \boldsymbol{\eta}' + \bar{\boldsymbol{u}} \times \boldsymbol{\eta}, \tag{A.6}$$

where $\boldsymbol{\eta}$ is defined through the relationship $\delta R = R[\boldsymbol{\eta}]_\times$.

Property Appendix A.1. *Let $\boldsymbol{q} \in \mathbb{R}^n$ and $R \in \mathcal{SO}(3)$, such that $R' = R[\bar{\boldsymbol{u}}]_\times$. We decompose R as $R = [\boldsymbol{d}_1, \boldsymbol{d}_2, \boldsymbol{d}_3]$, where $\boldsymbol{d}_j$ is the j^{th} column of the matrix R. We denote by $\mathbf{e}_j$ the j^{th} canonical vector of $\mathbb{R}^3$. We consider the Lagrangian $\mathring{\mathcal{L}}(\boldsymbol{q}, \boldsymbol{q}', R, \bar{\boldsymbol{u}})$. The Euler-Lagrange equations on $\mathbb{R}^n \times \mathcal{SO}(3)$ read*

$$\frac{\mathrm{d}}{\mathrm{d}s}\frac{\partial \mathcal{L}}{\partial \boldsymbol{q}'} + \frac{\mathrm{d}}{\mathrm{d}s}\frac{\partial \mathcal{L}}{\partial \bar{\boldsymbol{u}}} + [\bar{\boldsymbol{u}}]_\times \frac{\partial \mathcal{L}}{\partial \bar{\boldsymbol{u}}} - \frac{\partial \mathcal{L}}{\partial \boldsymbol{q}} - \sum_{j=1}^{3} [\mathbf{e}_j]_\times R^{\mathrm{T}} \frac{\partial \mathcal{L}}{\partial \boldsymbol{d}_j} = 0. \tag{A.7}$$

Proof:. Using properties of rotation matrices, we have $\boldsymbol{d}'_j = [R\,\bar{\boldsymbol{u}}]_\times \boldsymbol{d}_j = R[\bar{\boldsymbol{u}}]_\times R^{\mathrm{T}}\,\boldsymbol{d}_j$, and likewise, $\delta \boldsymbol{d}_j = R[\boldsymbol{\eta}]_\times R^{\mathrm{T}} \boldsymbol{d}_j$. The action of the system reads $S = \int_0^L \mathring{\mathcal{L}}(\boldsymbol{q}, \boldsymbol{q}', \boldsymbol{d}_j, \bar{\boldsymbol{u}})$. We search for a stationary point of S, that is trajectories $\boldsymbol{q}(s), R(s)$ of the system such that $\delta S = 0$.

We have

$$\begin{aligned} \delta S &= S(\boldsymbol{q}+\delta\boldsymbol{q}, \boldsymbol{q}'+\delta\boldsymbol{q}', \boldsymbol{d}_j+\delta\boldsymbol{d}_j, \bar{\boldsymbol{u}}+\delta\bar{\boldsymbol{u}}) - S(\boldsymbol{q}, \boldsymbol{q}', \boldsymbol{d}_j, \bar{\boldsymbol{u}}) && \text{(A.8)} \\ &= \underbrace{\int_0^L \frac{\partial \mathring{\mathcal{L}}}{\partial \boldsymbol{q}} \cdot \delta\boldsymbol{q} + \frac{\partial \mathring{\mathcal{L}}}{\partial \boldsymbol{q}'} \cdot \delta\boldsymbol{q}'}_{\delta S_{\mathrm{T}}} + \underbrace{\int_0^L \frac{\partial \mathring{\mathcal{L}}}{\partial \boldsymbol{d}_j} \cdot \delta\boldsymbol{d}_j + \frac{\partial \mathring{\mathcal{L}}}{\partial \bar{\boldsymbol{u}}} \cdot \delta\bar{\boldsymbol{u}}}_{\delta S_{\mathrm{R}}}\,. && \text{(A.9)} \end{aligned}$$

The first term S_{T} is classical: by using the permutation $\delta(\boldsymbol{q}') = (\delta\boldsymbol{q})'$ and integration by part with the boundary conditions (A.4) and (A.5), one obtains

$$\delta S_{\mathrm{T}} = \int_0^L \left(\frac{\mathrm{d}}{\mathrm{d}s} \frac{\partial \mathcal{L}}{\partial \boldsymbol{q}'} + \frac{\mathrm{d}}{\mathrm{d}s} \frac{\partial \mathcal{L}}{\partial \bar{\boldsymbol{u}}} \right) \cdot \delta\boldsymbol{q},$$

which, for any perturbation $\delta\boldsymbol{q}$, yields the classical Euler-Lagrange equations (A.1).

Now we compute the second term $\delta S_{\mathrm{R}} = \underbrace{\int_0^L \frac{\partial \mathring{\mathcal{L}}}{\partial \boldsymbol{d}_j} \cdot \delta\boldsymbol{d}_j}_{\delta S_{\mathbf{d}_j}} + \underbrace{\int_0^L \frac{\partial \mathring{\mathcal{L}}}{\partial \bar{\boldsymbol{u}}} \cdot \delta\bar{\boldsymbol{u}}}_{\delta S_{\bar{\boldsymbol{u}}}}$. On the one hand, using the compatibility equation (A.6), we have

$$\begin{aligned} \delta S_{\bar{\boldsymbol{u}}} &= \int_0^L \frac{\partial \mathring{\mathcal{L}}}{\partial \bar{\boldsymbol{u}}} \cdot \boldsymbol{\eta}' + \frac{\partial \mathring{\mathcal{L}}}{\partial \bar{\boldsymbol{u}}} \cdot ([\bar{\boldsymbol{u}}]_\times \boldsymbol{\eta}) \\ &= \int_0^L \frac{\partial \mathring{\mathcal{L}}}{\partial \bar{\boldsymbol{u}}} \cdot \boldsymbol{\eta}' - \left([\bar{\boldsymbol{u}}]_\times \frac{\partial \mathring{\mathcal{L}}}{\partial \bar{\boldsymbol{u}}} \right) \cdot \boldsymbol{\eta} && \text{using properties of the mixed product} \\ &= -\int_0^L \left(\frac{\mathrm{d}}{\mathrm{d}s} \frac{\partial \mathring{\mathcal{L}}}{\partial \bar{\boldsymbol{u}}} + [\bar{\boldsymbol{u}}]_\times \frac{\partial \mathring{\mathcal{L}}}{\partial \bar{\boldsymbol{u}}} \right) \cdot \boldsymbol{\eta} && \text{using integration by part and boundary conditions} \end{aligned}$$

$$\left[\frac{\partial \mathring{\mathcal{L}}}{\partial \bar{\boldsymbol{u}}} \cdot \boldsymbol{\eta} \right]_0^L = 0, \tag{A.10}$$

i.e.

$$\frac{\partial \mathring{\mathcal{L}}}{\partial \bar{\boldsymbol{u}}}(0) = 0 \quad \text{or } \boldsymbol{\eta}(0) = 0 \tag{A.11}$$

$$\frac{\partial \mathring{\mathcal{L}}}{\partial \bar{\boldsymbol{u}}}(L) = 0 \quad \text{or } \boldsymbol{\eta}(L) = 0, \tag{A.12}$$

meaning that either the infinitesimal rotation $\boldsymbol{\eta}$ or the applied angular momentum $\frac{\partial \mathcal{L}}{\partial \bar{\boldsymbol{u}}}$ cancels out at a boundary point.

On the other hand, we have

$$\begin{aligned} \delta S_{\mathbf{d}_j} &= \int_0^L \frac{\partial \mathring{\mathcal{L}}}{\partial \boldsymbol{d}_j} \cdot \delta\boldsymbol{d}_j \\ &= \int_0^L \frac{\partial \mathring{\mathcal{L}}}{\partial \boldsymbol{d}_j} \cdot \left([\boldsymbol{\eta}]_\times R^{\mathrm{T}} \boldsymbol{d}_j \right) \\ &= \int_0^L \frac{\partial \mathring{\mathcal{L}}}{\partial \boldsymbol{d}_j} \cdot \left([\boldsymbol{\eta}]_\times \mathbf{e}_j \right) && \text{where } \mathbf{e}_j \text{ is the } j^{\text{th}} \text{ vector of the canonical base on } \mathbb{R}^3 \\ &= \int_0^L \left([\mathbf{e}_j]_\times R^{\mathrm{T}} \frac{\partial \mathring{\mathcal{L}}}{\partial \boldsymbol{d}_j} \right) \cdot \boldsymbol{\eta} && \text{using properties of the mixed product.} \end{aligned}$$

We finally obtain

$$\delta S_{\bar{\boldsymbol{u}}} = \int_0^L \left(-\frac{\mathrm{d}}{\mathrm{d}s} \frac{\partial \mathring{\mathcal{L}}}{\partial \bar{\boldsymbol{u}}} - [\bar{\boldsymbol{u}}]_\times \frac{\partial \mathring{\mathcal{L}}}{\partial \bar{\boldsymbol{u}}} + \sum_{j=1}^{3} [\mathbf{e}_j]_\times R^{\mathrm{T}} \frac{\partial \mathring{\mathcal{L}}}{\partial \boldsymbol{d}_j} \right) \cdot \boldsymbol{\eta},$$

which, for any perturbation $\boldsymbol{\eta}$, yields the Euler-Lagrange equations on $\mathcal{SO}(3)$, in the local basis R,

$$\frac{\mathrm{d}}{\mathrm{d}s} \frac{\partial \mathring{\mathcal{L}}}{\partial \bar{\boldsymbol{u}}} + [\bar{\boldsymbol{u}}]_\times \frac{\partial \mathring{\mathcal{L}}}{\partial \bar{\boldsymbol{u}}} - \sum_{j=1}^{3} [\mathbf{e}_j]_\times R^{\mathrm{T}} \frac{\partial \mathring{\mathcal{L}}}{\partial \boldsymbol{d}_j} = 0,$$

or alternatively, in the world basis,

$$\frac{\mathrm{d}}{\mathrm{d}s} \left(R \frac{\partial \mathring{\mathcal{L}}}{\partial \bar{\boldsymbol{u}}} \right) - \sum_{j=1}^{3} [\boldsymbol{d}_j]_\times \frac{\partial \mathring{\mathcal{L}}}{\partial \boldsymbol{d}_j} = 0.$$

Summing up the $\mathbb{R}^n$ contribution together with this $\mathcal{SO}(3)$ contribution, one ends up with the general Euler-Lagrange equations (A.7) on $\mathbb{R}^n \times \mathcal{SO}(3)$. □

Appendix A.3. Noether's theorem on $\mathbb{R}^n \times \mathcal{SO}(3)$

Property Appendix A.2. *The Noether arclength invariant on $\mathbb{R}^n \times \mathcal{SO}(3)$, corresponding to a translational symmetry of $\mathring{\mathcal{L}}$ along s, reads*

$$\forall s, \quad \mathring{H}'(s) = 0 \qquad \text{with} \quad \mathring{H}(s) = \mathring{H} = \boldsymbol{q}' \frac{\partial \mathring{\mathcal{L}}}{\partial \boldsymbol{q}'} + \bar{\boldsymbol{u}} \frac{\partial \mathring{\mathcal{L}}}{\partial \bar{\boldsymbol{u}}} - \mathring{\mathcal{L}}. \tag{A.13}$$

Property Appendix A.3. *The Noether configuration rotation invariant on $\mathbb{R}^n \times \mathcal{SO}(3)$, corresponding to a rotation symmetry of $\mathring{\mathcal{L}}$ around $\boldsymbol{d}_3$, reads*

$$\left(\boldsymbol{\theta} \cdot \frac{\partial \mathring{\mathcal{L}}}{\partial \bar{\boldsymbol{u}}} \right)' = 0 \quad \forall s. \tag{A.14}$$

The proofs of these two properties are similar and follow from the Euler-Lagrange equations on $\mathbb{R}^n \times \mathcal{SO}(3)$ derived above. They contain two key steps: first, computing the total derivative of the Lagrangian $\mathring{\mathcal{L}}$; then replacing gradients of the form $\frac{\partial \mathring{\mathcal{L}}}{\partial \boldsymbol{q}}$ and $\frac{\partial \mathring{\mathcal{L}}}{\partial \boldsymbol{d}_j}$ by their expressions extracted from the Euler-Lagrange equations.

Appendix B. Planar Elastica statics, dynamics, and vibrations

The equations for the dynamics of the planar Elastica can be obtained as the Euler-Lagrange equations of the action (91) together with the constraints (90). We write

$$\frac{\partial \mathcal{L}_d^{2D}}{\partial \boldsymbol{q}} = \left(\frac{\partial \mathcal{L}_d^{2D}}{\partial \boldsymbol{q}'} \right)' + \left(\frac{\partial \mathcal{L}_d^{2D}}{\partial \dot{\boldsymbol{q}}} \right)^{\bullet} \tag{B.1}$$

with $\boldsymbol{q} = (x, y, \theta, \kappa)$ and obtain

$$x'(s,t) = \cos\theta\,,\ y'(s,t) = \sin\theta\,,\ EI\theta'(s,t) = m\,,\ m'(s,t) = n_x \sin\theta - n_y \cos\theta\,,\ n_x'(s,t) = \rho S\,\ddot{x}\,,\ n_y'(s,t) = \rho S\,\ddot{y} \tag{B.2}$$

The equations for the statics of the planar Elastica are then obtained by setting $\dot{x} = \ddot{x} = 0$ and $\dot{y} = \ddot{y} = 0$ in (B.2)

$$x_e'(s) = \cos\theta_e\,,\ y_e'(s) = \sin\theta_e\,,\ EI\theta_e'(s) = m_e\,,\ m_e'(s) = n_{xe} \sin\theta_e - n_{ye} \cos\theta_e\,,\ n_{xe}'(s) = 0\,,\ n_{ye}'(s) = 0 \tag{B.3}$$

And finally, the equations for the vibrations of the planar Elastica are obtained by considering the ansatz (92), which corresponds to small-amplitude vibrations around the nonlinear equilibrium $\boldsymbol{q}_e(s)$. This ansatz is injected into (B.2) while bearing in mind that (B.3) is fulfilled and that we only keep $O(\epsilon)$ terms. We obtain

$$\bar{x}' = -\bar{\theta}\sin\theta_e\,,\ \bar{y}' = \bar{\theta}\cos\theta_e\,,\ EI\bar{\theta}' = \bar{m}\,,\ \bar{m}' = \bar{n}_x \sin\theta_e - \bar{n}_y \cos\theta_e + \bar{\theta}\left(n_{xe}\cos\theta_e + n_{ye}\sin\theta_e\right) \tag{B.4a}$$

$$\bar{n}_x' = -\rho S\,\omega^2\,\bar{x}\,,\ \bar{n}_y' = -\rho S\,\omega^2\,\bar{y} \tag{B.4b}$$

References

Antman, S.S., 2004. Nonlinear problems of elasticity. 2nd ed., Springer-Verlag, New York. doi:10.1007/0-387-27649-1.

Audoly, B., van der Heijden, G., 2022. Analysis of cone-like singularities in twisted elastic ribbons. Journal of the Mechanics and Physics of Solids 171, 105131. doi:10.1016/j.jmps.2022.105131.

Audoly, B., Pomeau, Y., 2010. Elasticity and Geometry: from hair curls to the nonlinear response of shells. Oxford University Press.

Bigoni, D., Corso, F.D., Bosi, F., Misseroni, D., 2015. Eshelby-like forces acting on elastic structures: Theoretical and experimental proof. Mechanics of Materials 80, 368 – 374. doi:10.1016/j.mechmat.2013.10.009.

Borum, A., 2018. Manipulation and mechanics of thin elastic objects. Ph.D. thesis. University of Illinois at Urbana-Champaign.

Bosi, F., Misseroni, D., Dal Corso, F., Bigoni, D., 2014. An elastica arm scale. Proceedings of the Royal Society A: Mathematical, Physical and Engineering Sciences 470, 20140232. doi:10.1098/rspa.2014.0232.

Bustamante, C., Bryant, Z., Smith, S.B., 2003. Ten years of tension: single-molecule dna mechanics. Nature 421, 423–427. doi:10.1038/nature01405.

Casati, R., 2015. Quelques contributions à la modélisation numérique de structures élancées pour l'informatique graphique. Ph.D. thesis. Grenoble Alpes Universités.

Cazzolli, A., Dal Corso, F., 2024. The elastica sling. European Journal of Mechanics - A/Solids 105, 105273. doi:10.1016/j.euromechsol.2024.105273.

Chai, H., 1998. The post-buckling response of a bi-laterally constrained column. J. Mech. Phys. Solids 46, 1155–1181. doi:10.1016/S0022-5096(98)00004-0.

Charrondière, R., Bertails-Descoubes, F., Neukirch, S., Romero, V., 2020. Numerical modeling of inextensible elastic ribbons with curvature-based elements. Computer Methods in Applied Mechanics and Engineering 364, 112922. doi:10.1016/j.cma.2020.112922.

Charrondière, R., Neukirch, S., Bertails-Descoubes, F., 2024. Merci: Mixed curvature-based elements for computing equilibria of thin elastic ribbons. ACM Transactions on Graphics (TOG) 43, art. 160. doi:10.1145/3674502.

Clauvelin, N., Audoly, B., Neukirch, S., 2009. Matched asymptotic expansions for twisted elastic knots: a self-contact problem with non-trivial contact topology. Journal of the Mechanics and Physics of Solids 57, 1623–1656. doi:10.1016/j.jmps.2009.05.004.

Coleman, B.D., Swigon, D., 2000. Theory of supercoiled elastic rings with self-contact and its application to DNA plasmids. Journal of Elasticity 60, 173–221.

Crisfield, M.A., Jelenić, G., 1998. Objectivity of strain measures in the geometrically exact three-dimensional beam theory and its finite-element implementation. Proc. Royal Society of London, Series A 455, 1125–1147.

Dal Corso, F., Misseroni, D., Pugno, N.M., Movchan, A.B., Movchan, N.V., Bigoni, D., 2017. Serpentine locomotion through elastic energy release. Journal of The Royal Society Interface 14, 20170055. doi:10.1098/rsif.2017.0055.

Dias, M.A., Audoly, B., 2015. 'wunderlich, meet kirchhoff': A general and unified description of elastic ribbons and thin rods. Journal of Elasticity 119, 49–66. doi:10.1007/s10659-014-9487-0.

Dichmann, D., Li, Y., Maddocks, J., 1996. Hamiltonian formulations and symmetries in rod mechanics, in: Mesirov, J., Schulten, K., Sumners, D. (Eds.), Mathematical Approaches to Biomolecular Structure and Dynamics. Springer Verlag. volume 82 of *The IMA Volumes in Mathematics and Its Applications*, pp. 71–113. doi:10.1007/978-1-4612-4066-2_6.

Dick, A., 1981. Emmy Noether 1882-1935. Birkhauser. doi:10.1007/978-1-4684-0535-4. translated by H. I. Blocher.

Domokos, G., Holmes, P., Royce, B., 1997. Constrained Euler buckling. Journal of Nonlinear Science 7, 281–314. doi:10.1007/BF02678090.

Elettro, H., Grandgeorge, P., Neukirch, S., 2017. Elastocapillary coiling of an elastic rod inside a drop. Journal of Elasticity 127, 235–247. doi:10.1007/s10659-016-9611-4.

Hearle, J.W.S., 2014. The 20th-Century Revolution In Textile Machines And Processes. Part 2: Textured Yarns And Other Technologies. Industrial Archaeology Review 36, 32–47. doi:10.1179/0309072814Z.00000000028.

van der Heijden, G.H.M., Neukirch, S., Goss, V.G.A., Thompson, J.M.T., 2003. Instability and self-contact phenomena in the writhing of clamped rods. Int. J. Mech. Sci. 45, 161–196. doi:doi:10.1016/S0020-7403(02)00183-2.

Kehrbaum, S., Maddocks, J.H., 1997. Elastic rods, rigid bodies, quaternions and the last quadrature. Philosophical Transactions of the Royal Society of London. Series A, Mathematical and Physical Sciences 355, 2117–2136. doi:10.1098/rsta.1997.0113.

Keller, J., Niordson, F., 1966. The tallest column. Journal of Mathematics and Mechanics 16, 433–446.

Kienzler, R., Herrmann, G., 1986. On material forces in elementary beam theory. Journal of Applied Mechanics 53, 561–564. doi:10.1115/1.3171811.

Kirchhoff, G., 1859. Über das Gleichgewicht und die Bewegung eines unendlich dünnen elastischen Stabes. J. Reine Angew. Math. 56, 285–313.

Lee, T., Leok, M., McClamroch, N.H., 2018. Global Formulations of Lagrangian and Hamiltonian Dynamics on Manifolds. Interaction of Mechanics and Mathematics, Springer. doi:10.1007/978-3-319-56953-6.

Love, A.E.H., 1944. A Treatise on the Mathematical Theory of Elasticity. 4th ed. ed., Dover Publications, New York.

Lubinski, A., Althouse, W., 1962. Helical buckling of tubing sealed in packers. Journal of Petroleum Technology 14, 655–670. doi:10.2118/178-PA.

Maddocks, J.H., Dichmann, D.J., 1994. Conservation laws in the dynamics of rods. Journal of Elasticity 34, 83–96. doi:10.1007/BF00042427.

Manning, R.S., Bulman, G.B., 2005. Stability of an elastic rod buckling into a soft wall. Proceedings of the Royal Society A: Mathematical, Physical and Engineering Science 461, 2423–2450. doi:10.1098/rspa.2005.1458.

Neukirch, S., Audoly, B., 2021. A convenient formulation of Sadowsky's model for elastic ribbons. Proc. R. Soc. A 477, 20210548. doi:10.1098/rspa.2021.0548.

Noether, E., 1908. Über die Bildung des Formensystems der ternären biquadratischen Form. Journal fur die reine und angewandte Mathematik , 23–90.

Noether, E., 1918. Invariante variationsprobleme. Nachrichten von der Gesellschaft der Wissenschaften zu Göttingen. Mathematisch-Physikalische Klasse , 235–257.

Olver, P.J., 1984. Conservation laws in elasticity. Archive for Rational Mechanics and Analysis 85, 131–160. doi:10.1007/BF00281448.

O'Reilly, O.M., 2007. A material momentum balance law for rods. Journal of Elasticity 86, 155–172. doi:10.1007/s10659-006-9089-6.

O'Reilly, O.M., 2015. Some perspectives on eshelby-like forces in the elastica arm scale. Proceedings of the Royal Society A: Mathematical, Physical and Engineering Sciences 471, 20140785. doi:10.1098/rspa.2014.0785.

O'Reilly, O.M., 2017. Modeling Nonlinear Problems in the Mechanics of Strings and Rods: The Role of the Balance Laws. Interaction of Mechanics and Mathematics, Springer. doi:10.1007/978-3-319-50598-5.

Peng, W., Yun, X., Yu-Lu, L., 2013. Noether symmetry and conserved quantities of the analytical dynamics of a cosserat thin elastic rod. Chinese Physics B 22, 104503. doi:10.1088/1674-1056/22/10/104503.

Reissner, E., 1973. One one-dimensional large-displacement finite-strain beam theory. Studies in App. Math. 52, 87–95.

Roman, B., Pocheau, A., 1999. Buckling cascade of thin plates: Forms, constraints and similarity. Europhysics Letters (EPL) 46, 602–608. doi:10.1209/epl/i1999-00306-3.

Romero, I., Gebhardt, C.G., 2020. Variational principles for nonlinear Kirchhoff rods. Acta Mechanica 231, 625–647. doi:10.1007/s00707-019-02562-0.

Simo, J., Vu-Quoc, L., 1986. A three-dimensional finite-strain rod model. part ii: Computational aspects. Computer Methods in Applied Mechanics and Engineering 58, 79 – 116. URL: http://www.sciencedirect.com/science/article/pii/0045782586900794, doi:10.1016/0045-7825(86)90079-4.

Singh, H., Hanna, J.A., 2021. Pseudomomentum: origins and consequences. Zeitschrift für angewandte Mathematik und Physik 72, 122. doi:10.1007/s00033-021-01507-9.

Sonneville, V., Cardona, A., Brüls, O., 2014. Geometrically exact beam finite element formulated on the special Euclidean group. Computer Methods in Applied Mechanics and Engineering 268, 451–474. doi:10.1016/j.cma.2013.10.008.

Starostin, E.L., van der Heijden, G.H.M., 2015. Equilibrium shapes with stress localisation for inextensible elastic möbius and other strips. Journal of Elasticity 119, 67–112. doi:10.1007/s10659-014-9495-0.

Strick, T.R., Allemand, J.F., Bensimon, D., Bensimon, A., Croquette, V., 1996. The elasticity of a single supercoiled DNA molecule. Science 271, 1835–1837. doi:10.1126/science.271.5257.1835.

Thompson, J.M.T., van der Heijden, G.H.M., Neukirch, S., 2002. Supercoiling of dna plasmids: mechanics of the generalized ply. Proc. R. Soc. Lond. A 458, 959–985.